

**LOS ALAMOS SCIENTIFIC LABORATORY**  
**OF THE UNIVERSITY OF CALIFORNIA • LOS ALAMOS NEW MEXICO**

---

**LAGRANGIAN DIFFERENCE APPROXIMATIONS  
FOR FLUID DYNAMICS**

Index

✓ (1) Fluid Dynamics, Computations of  
flow with Shocks

✓ (2) Shocks in fluid flow, Lagrangian  
method of computation

201 III  
**DISTRIBUTION STATEMENT A**  
Approved for Public Release  
Distribution Unlimited

20000915 061

LA-2535  
PHYSICS  
TID-4500, 16th ed.

**LOS ALAMOS SCIENTIFIC LABORATORY**  
**OF THE UNIVERSITY OF CALIFORNIA    LOS ALAMOS    NEW MEXICO**

---

**REPORT WRITTEN:** March 1961

**REPORT DISTRIBUTED:** June 14, 1961

**LAGRANGIAN DIFFERENCE APPROXIMATIONS**  
**FOR FLUID DYNAMICS**

by

Jacob E. Fromm

This report expresses the opinions of the author or authors and does not necessarily reflect the opinions or views of the Los Alamos Scientific Laboratory.

Contract W-7405-ENG. 36 with the U. S. Atomic Energy Commission

## ABSTRACT

Various procedures are given for writing explicit difference approximations to the one-dimensional Lagrangian hydrodynamics equations. Computational comparisons are made among systems of equations with timing modifications. These comparisons lead to experimentally superior differencing forms. Stability analyses of these difference forms show the reasons for the superiority of one form over another. Of greater importance, the stability criteria obtained show the function of an artificially introduced diffusion term required in the treatment here given to shocks. The stability criterion in each case involves the familiar Courant condition and a term which corresponds to the stability criterion of the diffusion equation. Upper limits to the magnitude of the coefficient of the diffusion term are established as a function of Courant number. While lower limits are also indicated, they require modification when shocks are involved.

Alternate differencing schemes are considered in which the previously-used total energy calculation is replaced by an internal energy calculation. It is shown that care must be taken that the kinetic and internal energies are expressible in terms of local quantities. That is, in addition to the equations being conservative in a gross sense, they must also be locally conservative. This is necessary in order that the energy condition of the Rankine-Hugoniot equations be satisfied when shocks arise.

Finally discussion is given to errors resulting from the replacement of shocks by a shock layer, that is, errors connected with the artificially inserted diffusion term. These errors are manifested in distortions of profiles at material discontinuities through which shocks have passed and in rarefactions associated with such occurrences. The errors in turn effect stability in the vicinity of the material discontinuities.

## ACKNOWLEDGMENT

The author is indebted to Dr. Francis H. Harlow for his advice and assistance in all phases of this report. The theoretical aspects in particular were made possible through his guidance.

## TABLE OF CONTENTS

	Page
Abstract . . . . .	3
Chapter I.    Introduction to the Differencing Procedures. . . . .	7
Chapter II.   Computational Tests of Differencing Forms Involving Evaluation of Total Energy . . . . .	15
Chapter III.   Stability Analysis . . . . .	24
Chapter IV.   Differencing Procedures Involving the Internal Energy Calculation. . . . .	35
Chapter V.    Discussion of Errors . . . . .	44
References    . . . . .	49
Illustrations and Tables . . . . .	50
Appendix.    Entropy of a Region of Fluid . . . . .	66

## CHAPTER I

### INTRODUCTION TO THE DIFFERENCING PROCEDURES

#### The Differential Equations

The difference approximations discussed on the following pages are based upon the Lagrangian hydrodynamic equations written in conservative form<sup>1</sup> with  $t$ , the time, and  $m$ , the mass, as independent variables. The mass, momentum, and energy equations, respectively, are:

$$\frac{\partial(1/\rho)}{\partial t} - \frac{\partial u}{\partial m} = 0$$

$$\frac{\partial u}{\partial t} + \frac{\partial P}{\partial m} = 0$$

$$\frac{\partial E}{\partial t} + \frac{\partial(Pu)}{\partial m} = 0$$

The dependent variables characterizing the fluid are:

$\rho$  = density

$u$  = velocity

$P$  = pressure

$E$  = specific energy

The necessary additional equation is the equation of state.

The coordinate,  $x$ , of an element of fluid in the laboratory frame is a function of  $m$  and  $t$ . In terms of it the velocity is defined by

$$u = \frac{\partial x}{\partial t}$$

and through the mass equation it follows that

$$\frac{1}{\rho} = \frac{\partial x}{\partial m}$$

Some discussion will be given to the energy equation written in terms of the specific internal energy. This equation with mass and time as independent variables is

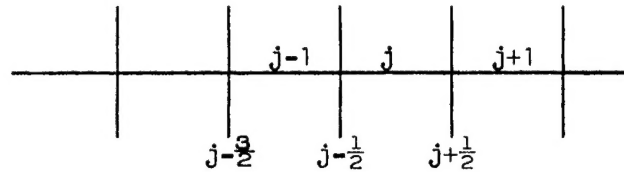
$$\frac{\partial I}{\partial t} + P \frac{\partial u}{\partial m} = 0$$

where

$$I = E - \frac{u^2}{2}$$

#### Differencing Procedures

To solve the initial-condition boundary-value problem, we replace the differential equations by a set of finite-difference approximations whereby solution proceeds by a set of purely algebraic operations. To accomplish this we represent the continuum of fluid by a set of "finite elements" of mass  $m_j$ , where  $j = 1, 2, 3 \dots j_0$  number the centers of mass of the elements or "cells." These elements are shown in the following diagram.



The Lagrangian equations relate the field variables at points moving with the fluid, so that points of information in the mesh of cells, whether they are centers of mass of the elements, ...  $j - 1$ ,  $j$ ,  $j + 1$  ..., or cell boundaries, ...  $j - 3/2$ ,  $j - 1/2$ ,  $j + 1/2$  ..., will include between them increments of mass which remain constant in time. In the following discussion we will refer to the centers of mass of the cells simply as cell centers. It should be noted that this does not in general correspond to the spacial cell center.

There is some arbitrariness in regard to the points where the field variables should be defined. Some must be defined both at cell centers and at cell boundaries. We describe a procedure in which points of information and the sequence of calculations are as follows:

1. Compute velocity changes at cell boundaries with the momentum equation.
2. Compute density changes at cell centers with the mass equation.
3. Compute energy changes at cell centers with the energy equation.
4. Compute cell center pressures with the equation of state.

In the process of differencing where the values of the field variables are required and are not given by the above, we use interpolation formulas.

We tentatively make a direct correspondence between the differential and the difference equations, that is, let

$$\frac{\partial u}{\partial t} = - \frac{\partial P}{\partial m} \longrightarrow \frac{u_{j-\frac{1}{2}}^{n+1} - u_{j-\frac{1}{2}}^n}{\Delta t} = - \frac{P_j^n - P_{j-1}^n}{\frac{1}{2}(m_j + m_{j-1})} \quad (1)$$

$$\frac{\partial x}{\partial t} = u \longrightarrow \frac{x_{j-\frac{1}{2}}^{n+1} - x_{j-\frac{1}{2}}^n}{\Delta t} = u_{j-\frac{1}{2}}^n \quad (2)$$

$$\frac{1}{\rho} = \frac{\partial x}{\partial m} \longrightarrow \rho_j^{n+1} = \frac{m_j}{x_{j+\frac{1}{2}}^{n+1} - x_{j-\frac{1}{2}}^{n+1}} \quad (3)$$

$$\frac{\partial E}{\partial t} = - \frac{\partial (Pu)}{\partial m} \longrightarrow \frac{E_j^{n+1} - E_j^n}{\Delta t} = - \frac{(Pu)_{j+\frac{1}{2}}^n - (Pu)_{j-\frac{1}{2}}^n}{m_j} \quad (4)$$

The superscripts  $n$  are used to designate time steps. Thus, for example,  $u^n$  represents  $u(n\Delta t)$ ,  $u^{n+1}$  represents  $u[(n+1)\Delta t]$ , etc.

To see more clearly what we have done in making the above correspondences of the differential and difference equations, assume a knowledge of the boundary velocity,  $u_{j-\frac{1}{2}}^n$ , and the boundary pressure,  $P_{j-\frac{1}{2}}^n$ , at time  $n$ . Then the other quantities in the momentum equation in terms of Taylor expansions are

$$u_{j-\frac{1}{2}}^{n+1} = u_{j-\frac{1}{2}}^n + \Delta t \left( \frac{\partial u}{\partial t} \right)_{j-\frac{1}{2}}^n + \frac{\Delta t^2}{2} \left( \frac{\partial^2 u}{\partial t^2} \right)_{j-\frac{1}{2}}^n + \dots$$

$$P_{j-1}^n = P_{j-\frac{1}{2}}^n - \frac{m_{j-1}}{2} \left( \frac{\partial P}{\partial m} \right)_{j-\frac{1}{2}}^n + \frac{m_{j-1}^2}{8} \left( \frac{\partial^2 P}{\partial m^2} \right)_{j-\frac{1}{2}}^n + \dots$$

$$P_j^n = P_{j-\frac{1}{2}}^n + \frac{m_j}{2} \left( \frac{\partial P}{\partial m} \right)_{j-\frac{1}{2}}^n + \frac{m_j^2}{8} \left( \frac{\partial^2 P}{\partial m^2} \right)_{j-\frac{1}{2}}^n + \dots$$

The pressure difference as it appears in the momentum equation is then

$$P_{j-1}^n - P_j^n = - \frac{m_{j-1} + m_j}{2} \left( \frac{\partial P}{\partial m} \right)_{j-\frac{1}{2}}^n + O(\Delta m^2)$$



or a first order approximation to the derivative is

$$-\left(\frac{\partial P}{\partial m}\right)_{j-\frac{1}{2}}^n = \frac{P_{j-1}^n - P_j^n}{\frac{1}{2}(m_{j-1} + m_j)} \quad (5)$$

Similarly a first order approximation to the time derivative of the velocity is given by

$$\left(\frac{\partial u}{\partial t}\right)_{j-\frac{1}{2}}^n = \frac{u_{j-\frac{1}{2}}^{n+1} - u_{j-\frac{1}{2}}^n}{\Delta t}$$

Replacing the differential equation by these approximations at the point  $j-\frac{1}{2}, n$  leads to

$$u_{j-\frac{1}{2}}^{n+1} = u_{j-\frac{1}{2}}^n + \frac{P_{j-1}^n - P_j^n}{\frac{1}{2}(m_{j-1} + m_j)} \Delta t \quad (6)$$

which is just the momentum equation (1) given above.

Note now that if we add the pressures  $P_j^n$  and  $P_{j-1}^n$  in the above expansions and replace the mass derivative of the pressure as specified by (5), then we have

$$P_j^n + P_{j-1}^n = 2P_{j-\frac{1}{2}}^n + \frac{m_{j-1} - m_j}{2} \frac{P_{j-1}^n - P_j^n}{\frac{1}{2}(m_{j-1} + m_j)} + O(\Delta m^2)$$

Thus a first order approximation to the boundary pressure is

$$P_{j-\frac{1}{2}}^n = \frac{m_j P_{j-1}^n + m_{j-1} P_j^n}{m_j + m_{j-1}} \quad (7)$$

This equation provides one of the necessary interpolation formulas since the cell boundary pressures are required in equation (4).

A similar treatment of the mass equation leads to an interpolation

formula for cell center velocities, namely,

$$u_j^n = \frac{u_{j+\frac{1}{2}}^n + u_{j-\frac{1}{2}}^n}{2} \quad (8)$$

Although the necessity for such an interpolation formula is not indicated in the above, we shall need to evaluate the material pressure as a function of internal energy, which in turn is obtained by

$$I_j^n = E_j^n - \frac{\left(u_j^n\right)^2}{2}$$

In the examples here discussed the polytropic gas equation of state is used, i.e.,

$$P_m = (\gamma - 1)\rho I \quad (9)$$

The subscript m is used to distinguish the material pressure obtained through the equation of state from the total pressure P which includes a quantity q called the "psuedo-viscous pressure;"<sup>2</sup> that is

$$P = P_m + q \quad (10)$$

The term q is introduced into the equations to spread shock fronts and "smooth" computational results. The spread of shock fronts to a thickness on the order of the mesh spacing avoids the necessity for special treatment of shocks in the difference approximation. The effect of q must be such that shock speed and jump in the field variables across

the front are correct. This is not in general difficult to achieve. The Rankine-Hugoniot jump condition equations are merely statements of "local" conservation of mass, energy, and momentum, that is, they are statements of the conservation laws across the shock. Hence, if the system of difference equations is "locally" conservative, then the Rankine-Hugoniot conditions are satisfied and the treatment will be correct except for the spread of the shock front. Some further discussion of this will be given later in connection with computational experiments.

Smoothing of fluctuations through the use of  $q$  has bearing upon the stability of the difference equations. Considerable discussion of this will be given in Chapter III. In those cases where the system of equations is unconditionally unstable, the addition of  $q$  can make the system conditionally stable. If the system is conditionally stable without  $q$ , the smoothing effect is still desirable.

The form of  $q$  here considered is<sup>3</sup>

$$\begin{aligned} q_j^n &= \lambda \rho_j^n C_j^n \left( u_{j-\frac{1}{2}}^n - u_{j+\frac{1}{2}}^n \right) & \text{if } u_{j-\frac{1}{2}}^n - u_{j+\frac{1}{2}}^n > 0 \\ q_j^n &= 0 & \text{if } u_{j-\frac{1}{2}}^n - u_{j+\frac{1}{2}}^n \leq 0 \end{aligned} \quad (11)$$

$C$  is the material sound speed and  $\lambda$  is a constant, the magnitude of which is discussed in detail in Chapter III. Note that  $q$  is set to zero if the material is in a process of expanding. The desirability of this will be discussed further in Chapter V in connection with effects upon rarefactions.

Tentative to the discussion in Chapter III, the Courant condition

$$C \frac{\Delta t}{\Delta x} < 1$$

will be used as a measure of stability. That is, we will require

$$\left( \frac{C}{\Delta x} \right)_{\max} \Delta t < 1$$

In places where this measure of stability is used to control the time increment, violations of the true stability conditions may occur, but these will be localized and temporary.

## CHAPTER II

### COMPUTATIONAL TESTS OF DIFFERENCING FORMS INVOLVING EVALUATION OF TOTAL ENERGY\*

Prior to testing by computation any particular form of differencing, it is always important to examine the character of the error terms arising in the differencing procedure. Usually it is desirable that the error terms vanish for infinitesimal space and time increments. The types of differencing considered here all come under this category provided that certain stability criteria are satisfied. [Note: For discussion of a method of accuracy analysis the reader is referred to Reference 4 by Harlow p. 11 ff].

In establishing what, in the form of computational results, characterizes a good differencing scheme, it is helpful to have an analytic solution of some simplified problem for comparison. If no such solution is known, an alternative basis for comparison is a result obtained with

---

\*This is in contrast to difference forms in which the internal energy is evaluated, and the total energy is treated as an auxiliary quantity. Such forms will be discussed in Chapter IV.

a highly refined mesh, that is, a solution common to all differencing forms under consideration. If the difference approximation represents well some of the more important functionals, then more stringent criteria may be applied. Practical considerations require that we have as much accuracy as possible in a coarse mesh. These considerations are: (1) The use of a minimum number of space mesh points to reduce storage requirements and thus also reduce calculation time per cycle. (2) The use of a minimum number of time cycles to reduce the over-all calculation time. Hence a loss of accuracy in a coarse mesh may be used as a device to eliminate some differencing forms.

A final computational criterion that may be used is a comparison in smoothness of results, that is, a comparison of the rate at which fluctuations damp. If a smoothing mechanism is involved, as in the present discussion, it must be the same for those difference forms to be compared. In using this criterion we are basically looking for a system of difference equations which possesses error terms that contribute to smoothness without affecting the accuracy of the over-all result.

The physical situation considered in the following tests is that of two materials; the material on the left, the energy source, is isothermal and its temperature or internal energy is specified. Energy flows from this material into an initially cold, heavier material. A shock wave moves into the initially cold material and a rarefaction moves into the isothermal material.

### First Test

We begin with the system of difference equations developed in Chapter I and concentrate on modifications of equation (2). Equation (2) again is

$$x_{j-\frac{1}{2}}^{n+1} = x_{j-\frac{1}{2}}^n + u_{j-\frac{1}{2}}^n \Delta t \quad (12)$$

We compare it with

$$x_{j-\frac{1}{2}}^{n+1} = x_{j-\frac{1}{2}}^n + \frac{u_{j-\frac{1}{2}}^n + u_{j-\frac{1}{2}}^{n+1}}{2} \Delta t \quad (13)$$

and

$$x_{j-\frac{1}{2}}^{n+1} = x_{j-\frac{1}{2}}^n + u_{j-\frac{1}{2}}^{n+1} \Delta t \quad (14)$$

The system of difference forms as a whole with the above modifications is relatively poor; our present objective is only to demonstrate which of (12), (13) and (14) is the best. The results of comparisons clearly showed that (14) was superior on the basis of the discussed considerations. This was first evident in calculations where the size of  $\Delta t$  was controlled by the Courant condition, that is, where the time step size was adjusted to satisfy  $C/\Delta x_{\max} \Delta t < 1$ . If for any time step this condition was violated,  $\Delta t$  was reduced by half and the calculation was repeated. On the other hand, if we everywhere had  $C/\Delta x \Delta t < \frac{1}{2}$ , then  $\Delta t$

was doubled on the following time step. The order of largest to smallest time step assumed in the three calculations was (14), (13) and (12). Thus in (12) and (13) there was a greater tendency toward fluctuations which in turn resulted in more violations of the Courant condition. The more coarse time mesh possible with (14) indicated that it was the more desirable form.

Further confidence was obtained in this conclusion by comparing the three forms at the same fixed  $\Delta t$ . Typical velocity profiles along with the theoretical curve are shown in Figure 1. Details of initial conditions are given in Table 1. The plot of the rarefaction to the left of cell 1 is rather poorly represented in terms of Lagrangian mesh points but was of no interest since it was the same in all cases. The relative magnitudes of the fluctuations in the region of the initially cold material through which the shock has passed (cell 1 and to the right) clearly indicate that form (14) has the least fluctuation.

Note that (12) is a truncation of the Taylor expansion

$$x_{j-\frac{1}{2}}^{n+1} = x_{j-\frac{1}{2}}^n + \Delta t \left( \frac{\partial x}{\partial t} \right)_{j-\frac{1}{2}}^n + \frac{\Delta t^2}{2} \left( \frac{\partial^2 x}{\partial t^2} \right)_{j-\frac{1}{2}}^n + O(\Delta t^3)$$

and (14) is a truncation of

$$x_{j-\frac{1}{2}}^{n+1} = x_{j-\frac{1}{2}}^n + \Delta t \left( \frac{\partial x}{\partial t} \right)_{j-\frac{1}{2}}^{n+1} - \frac{\Delta t^2}{2} \left( \frac{\partial^2 x}{\partial t^2} \right)_{j-\frac{1}{2}}^{n+1} + O(\Delta t^3)$$



Note also that

$$\frac{u^n + u^{n+1}}{2}$$

implies a velocity at some time between  $n$  and  $n + 1$ . If terms of second order in  $\Delta t$  are omitted,

$$\left(\frac{\partial x}{\partial t}\right)^{n+\frac{1}{2}} = \frac{u^n + u^{n+1}}{2}$$

By a Taylor expansion about  $n + \frac{1}{2}$ ,

$$\begin{aligned} x_{j-\frac{1}{2}}^{n+1} &= x_{j-\frac{1}{2}}^{n+\frac{1}{2}} + \frac{\Delta t}{2} \left(\frac{\partial x}{\partial t}\right)_{j-\frac{1}{2}}^{n+\frac{1}{2}} + \frac{\Delta t^2}{8} \left(\frac{\partial^2 x}{\partial t^2}\right)_{j-\frac{1}{2}}^{n+\frac{1}{2}} + O(\Delta t^3) \\ x_{j-\frac{1}{2}}^n &= x_{j-\frac{1}{2}}^{n+\frac{1}{2}} - \frac{\Delta t}{2} \left(\frac{\partial x}{\partial t}\right)_{j-\frac{1}{2}}^{n+\frac{1}{2}} + \frac{\Delta t^2}{8} \left(\frac{\partial^2 x}{\partial t^2}\right)_{j-\frac{1}{2}}^{n+\frac{1}{2}} - O(\Delta t)^3 \end{aligned}$$

hence (13) is a truncation of

$$x_{j-\frac{1}{2}}^{n+1} = x_{j-\frac{1}{2}}^n + \Delta t \left(\frac{\partial x}{\partial t}\right)_{j-\frac{1}{2}}^{n+\frac{1}{2}} + O(\Delta t^3)$$

We note that the lowest order error terms in (12) and (14) are second order, whereas in the case of (13) the lowest order error is of third order. From this point of view we conclude that form (13) should have given the best results. The fact that (14) gave the best results can be explained by the second order error having added a contribution to the smoothing of the results. A more satisfactory point of view, however, is one involving a relabeling of the equations such that the time index on

$u$  is everywhere reduced by  $1/2$ . This requires a revision of the initial conditions on  $u$  and we specify  $u^{-\frac{1}{2}} = 0$ . In revised form the equations (1), (14), and (4) become

$$u_{j-\frac{1}{2}}^{n+\frac{1}{2}} = u_{j-\frac{1}{2}}^{n-\frac{1}{2}} + \frac{P_{j-1}^n - P_j^n}{\frac{1}{2}(m_{j-1} + m_j)} \Delta t \quad (15)$$

$$x_{j-\frac{1}{2}}^{n+1} = x_{j-\frac{1}{2}}^n + u_{j-\frac{1}{2}}^{n+\frac{1}{2}} \Delta t \quad (16)$$

$$E_j^{n+1} = E_j^n + \frac{(P^n u^{n-\frac{1}{2}})_{j-\frac{1}{2}} - (P^n u^{n-\frac{1}{2}})_{j+\frac{1}{2}}}{m_j} \Delta t \quad (17)$$

This revision in the time index on  $u$  now makes the magnitude of the lowest order error in (12), (13), and (14) consistent with the computational results. Note also that the momentum equation (15) is now time-centered and is correct to third order in  $\Delta t$ .

The density equation (3) has remained unchanged, but the revised time index on  $u$  must be taken into account in the  $q$  equation (11) which now becomes

$$\begin{aligned} q_j^n &= \lambda \rho_j^n C_j^n \left( u_{j-\frac{1}{2}}^{n-\frac{1}{2}} - u_{j+\frac{1}{2}}^{n-\frac{1}{2}} \right) & \text{if } \left( u_{j-\frac{1}{2}}^{n-\frac{1}{2}} - u_{j+\frac{1}{2}}^{n-\frac{1}{2}} \right) > 0 \\ q_j^n &= 0 & \text{if } \left( u_{j-\frac{1}{2}}^{n-\frac{1}{2}} - u_{j+\frac{1}{2}}^{n-\frac{1}{2}} \right) \leq 0 \end{aligned} \quad (18)$$

Compensation could be made for the time shift in initial conditions on  $u$ , but this is not necessary since the effect is negligible.

### Second Test

Our basic equations for further experimentation are now those with the revised time index on  $u$ , and we proceed by considering modifications of equation (17). We compare it with

$$E_j^{n+1} = E_j^n + \frac{(P^n u^n)_{j-\frac{1}{2}} - (P^n u^n)_{j+\frac{1}{2}}}{m_j} \Delta t \quad (19)$$

and

$$E_j^{n+1} = E_j^n + \frac{(P^n u^{n+\frac{1}{2}})_{j-\frac{1}{2}} - (P^n u^{n+\frac{1}{2}})_{j+\frac{1}{2}}}{m_j} \Delta t \quad (20)$$

where  $u^n$  is now defined by

$$u^n \equiv \frac{u^{n+\frac{1}{2}} + u^{n-\frac{1}{2}}}{2} \quad (21)$$

In all of these cases we consider  $I_j^n$  and  $I_j^{n+1}$  as

$$I_j^n = E_j^n - \frac{(u_j^n)^{n-\frac{1}{2}}}{2}$$
$$I_j^{n+1} = E_j^{n+1} - \frac{(u_j^n)^{n+\frac{1}{2}}}{2}$$

The same initial conditions of the first test were again used, and the Courant condition was used to control the  $\Delta t$ .

Figure 2 is a plot of the velocity of the interface between the two materials. Note the continued oscillations in the case of equation (17) even at late times. Equations (19) and (20) show rapid damping of initial fluctuations, the velocity becoming the analytical value in a short

number of time cycles.[For details of the calculation refer to Table 2].

On the basis of the results as demonstrated by Figure 2, equation (17) was eliminated. To contrast (19) and (20) more precisely, Figure 3 is included. This is a typical late-time density profile taken from the same calculations. For the present we ignore the error in the cells near the material boundary and note that the fluctuations that are present with form (19) tend to average about the profile of form (20). The greater smoothness of (20) hence indicates that it is the more desirable form to use.

To summarize, consider the following chart in which the time indices on u are used to specify the types of variations of differencing forms which we have studied. The indices refer, respectively, to the first and second tests.

$n-\frac{1}{2}, n-\frac{1}{2}$	$n, n-\frac{1}{2}$	$n+\frac{1}{2}, n-\frac{1}{2}$
$n-\frac{1}{2}, n$	$n, n$	$n+\frac{1}{2}, n$
$n-\frac{1}{2}, n+\frac{1}{2}$	$n, n+\frac{1}{2}$	$n+\frac{1}{2}, n+\frac{1}{2}$

The first test was the upper row and the second test the right hand column. Our conclusions were that the combination  $n + \frac{1}{2}, n + \frac{1}{2}$  was the best form, that being the form where the position equation and the energy equation both used the most advanced time on the velocity.

Four of the nine variations in differencing listed above were not tried to this point. To double-check our conclusions the  $n, n$  and  $n, n + \frac{1}{2}$  forms were applied to the same problem. These forms both

proved to be poorer than both the  $n + \frac{1}{2}$ ,  $n$  and the  $n + \frac{1}{2}$ ,  $n + \frac{1}{2}$  forms. This indicated that there probably was no need to check the remaining two forms, and analysis of the next chapter confirms this.

## CHAPTER III

### STABILITY ANALYSIS

We are interested in performing stability analyses of the difference forms discussed in Chapter II. To include all these forms we incorporate a coefficient  $n + \alpha$  on  $u$  in the position equation, and a coefficient  $n + \beta$  on  $u$  in the energy equation, where  $\alpha$  and  $\beta$  may take on values  $-\frac{1}{2}$ ,  $0$ , and  $\frac{1}{2}$ . For simplicity we consider one material of equal cell masses. The system of equations under consideration then becomes

$$u_{j-\frac{1}{2}}^{n+\frac{1}{2}} = u_{j-\frac{1}{2}}^{n-\frac{1}{2}} + \frac{\delta t}{m} (P_{j-1}^n - P_j^n) \quad (22)$$

$$x_{j-\frac{1}{2}}^{n+1} = x_{j-\frac{1}{2}}^n + u_{j-\frac{1}{2}}^{n+\alpha} \delta t \quad (23)$$

$$\rho_j^n = \frac{m}{x_{j+\frac{1}{2}}^n - x_{j-\frac{1}{2}}^n} \quad (24)$$

$$I_j^{n+1} = I_j^n + \frac{\delta t}{m} \left[ (P^n u^{n+\beta})_{j-\frac{1}{2}} - (P^n u^{n+\beta})_{j+\frac{1}{2}} \right] - \left[ \frac{(u_{j-\frac{1}{2}}^{n+\frac{1}{2}} + u_{j+\frac{1}{2}}^{n+\frac{1}{2}})^2}{8} - \frac{(u_{j-\frac{1}{2}}^{n-\frac{1}{2}} + u_{j+\frac{1}{2}}^{n-\frac{1}{2}})^2}{8} \right] \quad (25)$$

$$q_j^n = \lambda \rho_j C_j^n \left( u_{j-\frac{1}{2}}^{n-\frac{1}{2}} - u_{j+\frac{1}{2}}^{n-\frac{1}{2}} \right) \quad (26)$$

For simplicity in the first analysis we are not restricting  $q$  as in (11).

Assume all quantities vary slightly from steady state values; that is, let

$$\begin{aligned} u_j &= u_0(1 + \xi_j) & \xi &\ll 1 \\ \rho_j &= \rho_0(1 + \epsilon_j) & \epsilon &\ll 1 \\ I_j &= I_0(1 + \delta_j) & \delta &\ll 1 \end{aligned} \quad (27)$$

Then through the equation of state we have for first variations of  $C$  and  $P_m$

$$\begin{aligned} C_j^n &= \sqrt{\gamma(\gamma-1)} I_j^n = C_0 \left( 1 + \frac{1}{2} \delta_j^n \right) \\ (P_m)_j^n &= (\gamma - 1) \rho_0 I_0 \left( 1 + \epsilon_j^n + \delta_j^n \right) \end{aligned}$$

The first variation of  $q$  is given by

$$q_j^n = \lambda \rho_0 C_0 u_0 \left( \xi_{j-\frac{1}{2}}^{n-\frac{1}{2}} - \xi_{j+\frac{1}{2}}^{n-\frac{1}{2}} \right)$$

The cell mass remains constant; hence

$$m = \rho \delta x = \rho_0 \delta x_0$$

We also define the Courant number

$$u \equiv \frac{C_0 \delta t}{\delta x_0}$$

Then the first variations of the momentum, mass, and energy equations, respectively, become

$$\begin{aligned} \left( \zeta_{j-\frac{1}{2}}^{n+\frac{1}{2}} - \zeta_{j-\frac{1}{2}}^{n-\frac{1}{2}} \right) &= \frac{c_0}{u_0} \frac{\mu}{\gamma} \left[ \left( \epsilon_{j-1}^n - \epsilon_j^n \right) + \left( \delta_{j-1}^n - \delta_j^n \right) \right] \\ &+ \lambda \mu \left[ \left( \zeta_{j-\frac{3}{2}}^{n-\frac{1}{2}} - \zeta_{j-\frac{1}{2}}^{n-\frac{1}{2}} \right) - \left( \zeta_{j-\frac{1}{2}}^{n-\frac{1}{2}} - \zeta_{j+\frac{1}{2}}^{n-\frac{1}{2}} \right) \right] \end{aligned} \quad (28)$$

$$\left( \epsilon_j^{n+1} - \epsilon_j^n \right) = \frac{u_0}{c_0} \mu \left( \zeta_{j-\frac{1}{2}}^{n+\alpha} - \zeta_{j+\frac{1}{2}}^{n+\alpha} \right) \quad (29)$$

$$\left( \delta_j^{n+1} - \delta_j^n \right) = (\gamma - 1) \frac{u_0}{c_0} \mu \left( \zeta_{j-\frac{1}{2}}^{n+\beta} - \zeta_{j+\frac{1}{2}}^{n+\beta} \right) \quad (30)$$

We now assume that the solution of these equations can be written in terms of a Fourier series. If this is true, then each term of the series is also a solution, and we may examine a typical one to note what the conditions are that would make it a solution. Assume that

$$\begin{aligned} \zeta_j^n &= \zeta e^{ikj_r n} \\ \epsilon_j^n &= \epsilon e^{ikj_r n} \\ \delta_j^n &= \delta e^{ikj_r n} \end{aligned} \quad (31)$$

Substitution of (31) into equations (28), (29), and (30) leads respectively, to the equations



$$\left(2i \frac{c_0}{u_0} \frac{\mu}{\gamma} \sin \frac{k}{2}\right) \epsilon + \frac{1}{\sqrt{r}} \left[(r-1) + 4 \lambda \mu \sin^2 \frac{k}{2}\right] \zeta + \left(2i \frac{c_0}{u_0} \frac{\mu}{\gamma} \sin \frac{k}{2}\right) \delta = 0$$

$$(r-1) \epsilon + \left(2i \frac{u_0}{c_0} \mu r^\alpha \sin \frac{k}{2}\right) \zeta = 0 \quad (32)$$

$$\left[2i(\gamma-1) \frac{u_0}{c_0} \mu r^\beta \sin \frac{k}{2}\right] \zeta + (r-1) \delta = 0$$

Then (31) is a solution provided that

$$D = \begin{vmatrix} 2i \frac{c_0}{u_0} \frac{\mu}{\gamma} \sin \frac{k}{2} & \frac{1}{\sqrt{r}} \left[(r-1) + 4 \lambda \mu \sin^2 \frac{k}{2}\right] & 2i \frac{c_0}{u_0} \frac{\mu}{\gamma} \sin \frac{k}{2} \\ (r-1) & 2i \frac{u_0}{c_0} \mu r^\alpha \sin \frac{k}{2} & 0 \\ 0 & 2i(\gamma-1) \frac{u_0}{c_0} \mu r^\beta \sin \frac{k}{2} & (r-1) \end{vmatrix} = 0 \quad (33)$$

or

$$(r-1) \left[(r-1) + 4 \lambda \mu \sin^2 \frac{k}{2}\right] + \frac{4 \mu^2 \sin^2 \frac{k}{2}}{\gamma} \left[r^{\alpha+\frac{1}{2}} + (\gamma-1) r^{\beta+\frac{1}{2}}\right] = 0 \quad (34)$$

For stability it is necessary that the typical component solution (31) not grow without bound. We therefore require that

$$|r| \leq 1 \quad (35)$$

We further require that (35) be satisfied in the extreme case of  $\sin^2 k/2 = 1$ ; this geometrically implies, for example, that if  $k = \pi$  the wave length of the typical component solution under consideration is just twice the cell size. Under these conditions it is possible for this component of each of the field variables to attain extreme maximum and minimum values in alternate cells, and the largest possible gradients can exist.

With these considerations we wish to solve for  $r$  the equation

$$(r - 1) [(r - 1) + 4 \lambda \mu] + \frac{4 \mu^2}{\gamma} \left[ r^{\alpha + \frac{1}{2}} + (\gamma - 1) r^{\beta + \frac{1}{2}} \right] = 0 \quad (36)$$

We shall confine our attention to those values of  $\alpha$  and  $\beta$  which lead to a quadratic equation in  $r$ . These cases are the ones which appear at the corners of the chart on Page 22. They are

$$\alpha = \beta = -\frac{1}{2}$$

$$\alpha = -\frac{1}{2}, \beta = \frac{1}{2}$$

$$\alpha = \frac{1}{2}, \beta = -\frac{1}{2}$$

$$\alpha = \beta = \frac{1}{2}$$

In all of these cases the equation reduces to a form

$$(r - 1)^2 + 4\mu a(r - 1) + 4\mu^2 = 0 \quad (36a)$$

where  $a$  is a function of  $\lambda$  and  $\mu$ . The forms of  $a$  for the four cases under consideration are:

$\alpha = \beta = -\frac{1}{2}$	$\alpha = \frac{1}{2}, \beta = -\frac{1}{2}$
$a = \lambda$	$a = \lambda + \frac{\mu}{\gamma}$
$\alpha = -\frac{1}{2}, \beta = \frac{1}{2}$	$\alpha = \beta = \frac{1}{2}$
$a = \lambda + \frac{\gamma - 1}{\gamma} \mu$	$a = \lambda + \mu$

Solved for  $r$ , equation (36a) becomes

$$r = 1 - 2\mu \left[ a \pm \sqrt{a^2 - 1} \right] \quad (37)$$

Now if  $a < 1$ ,  $r$  is imaginary and

$$|r| = \sqrt{1 - 4\mu(a - \mu)}$$

Thus the condition  $|r| \leq 1$  requires  $\mu \leq a$ .

If  $a = 1$ , then  $|r| \leq 1$  requires  $0 \leq \mu \leq 1$ . Here the lower limit is always satisfied while the upper limit is included for  $a < 1$ .

For  $a > 1$  we must examine both the plus and minus sign in the equation

$$r = 1 - 2\mu a \pm 2\mu \sqrt{a^2 - 1} \quad (38)$$

If the plus sign satisfies  $r \leq 1$ , then the minus sign will also. With the plus sign,  $r \leq 1$  requires that

$$-a + \sqrt{a^2 - 1} \leq 0$$

for  $\mu > 0$ . Note that this is always satisfied, since  $a$  is real.

If the minus sign in (38) satisfies  $r \geq -1$ , then the plus sign will also. Then  $r \geq -1$  requires that

$$\mu(a + \sqrt{a^2 - 1}) \leq 1.$$

This may also be written as a dual condition,

$$2a\mu - \mu^2 \leq 1 \text{ and } \mu < 1$$

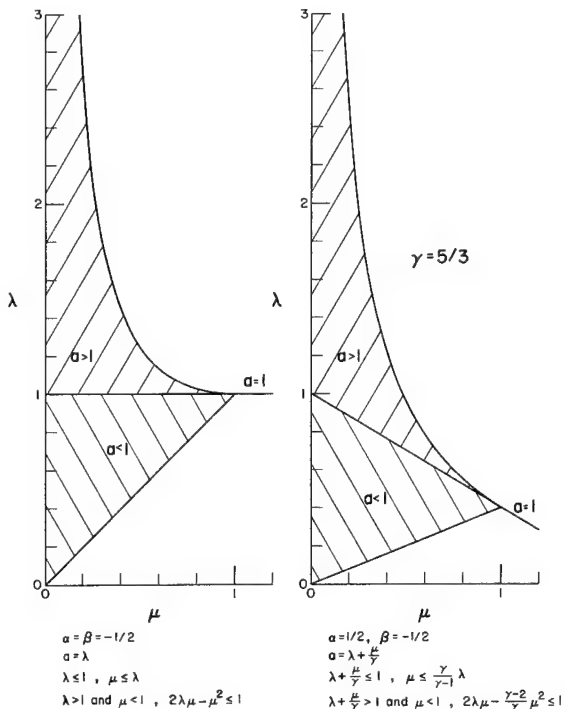
To summarize then, the conditions for stability are

For  $a \leq 1$ ,  $\mu \leq a$

For  $a > 1$  and  $\mu < 1$ ,  $2a\mu - \mu^2 \leq 1$

(39)

Plots of the regions of stability are given for the cases considered. Note that the forms of differencing that were experimentally superior are those for which the region of stability is shifted to the lowest values of  $\lambda$ . Qualitatively the inference is that the magnitude of  $q$ , and hence the degree of entropy increase introduced, must compensate for certain of the error terms that are inherent in a given system of difference equations. If the error terms are of the type that



cause an entropy decrease, they lead to fluctuations and hence require more compensation in the form of the dissipative mechanism  $q$ . [For further discussion of the relation between the entropy of a region and fluctuations the reader is referred to the Appendix.]

It is interesting to note that the introduction of  $q$  into the system of equations is equivalent to adding a diffusion term to the momentum equation. That is,

$$\frac{\partial u}{\partial t} = - \frac{\partial P}{\partial m} + \frac{\partial}{\partial m} (\lambda \rho C \delta m \frac{\partial u}{\partial m})$$

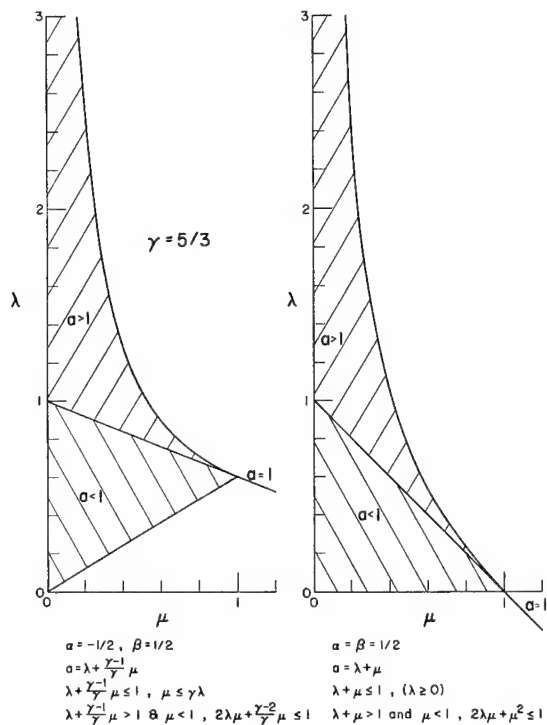
where  $\lambda \rho C \delta m$  is the diffusion coefficient. The stability criterion for the diffusion equation with this coefficient is

$$\lambda \rho C \delta m \frac{\delta t}{\delta m} \leq \frac{1}{2}$$

which reduces to

$$2\lambda\mu \leq 1$$

Thus it is seen that the stability conditions given above, relating to the upper limit on  $\lambda$ , all contain two terms, one connected with the



hydrodynamic equations, the other with the added diffusion. Only in the case  $\alpha = \beta = \frac{1}{2}$  are the equations conditionally stable without any added diffusion, i.e.,  $\lambda = 0$ . It will be noted that in this case the hydrodynamic term alone is just the Courant condition.

In the above analysis we did not consider the dissipative mechanism in the sense specified in Chapter II. That is,

$$q_j^n = 0 \quad \text{for } u_{j-\frac{1}{2}}^{n-\frac{1}{2}} - u_{j+\frac{1}{2}}^{n-\frac{1}{2}} \leq 0$$

To extend the analysis to this restricted  $q$ , we consider a typical cell interface velocity and assume that the most extreme fluctuations in this velocity arise from the existence of a viscous pressure to the left at one time cycle, and a viscous pressure to the right on the next time cycle. Let  $r_1$  refer to the times for which the viscous pressure is from the left, and  $r_2$  to the times for which the viscous pressure is from the right. Then stability at time  $n$  requires that

$$\left| r_1^{n/2} \quad r_2^{n/2} \right| \leq 1$$

or

$$\left| r_1 \quad r_2 \right| \leq 1 \quad (40)$$

The equations of first variation of  $\delta q$  for the cases  $r_1$  and  $r_2$  become, respectively,

$$\delta q = q_{j-1}^n = \lambda \rho \, c_0 u_0 \left( \zeta_{j-\frac{3}{2}}^{n-\frac{1}{2}} - \zeta_{j-\frac{1}{2}}^{n-\frac{1}{2}} \right)$$

$$\delta q = -q_j^n = -\lambda \rho c_0 u_0 \left( \zeta_{j-\frac{1}{2}}^{n-\frac{1}{2}} - \zeta_{j+\frac{1}{2}}^{n-\frac{1}{2}} \right)$$

The trial solution leads, respectively, to

$$\begin{aligned} \frac{\delta t}{\rho_0 \delta x_0} q_{j-1} &= \lambda \mu \frac{u_0}{c_0} e^{ik(j-\frac{1}{2})} \frac{r^n}{\sqrt{r}} (e^{ik} - 1) \zeta \\ - \frac{\delta t}{\rho_0 \delta x_0} q_j &= -\lambda \mu \frac{u_0}{c_0} e^{ik(j-\frac{1}{2})} \frac{r^n}{\sqrt{r}} (1 - e^{ik}) \zeta \end{aligned}$$

Then  $\delta q$  is the same for  $r_1$  and  $r_2$ , and the stability criteria

$$|r| < 1$$

again applies but now with  $\lambda$  replaced by  $\lambda/2$ . Thus the stability conditions for the four forms of differencing discussed above become:

$\alpha = \beta = -\frac{1}{2}$ $a = \frac{\lambda}{2}$	$\alpha = \frac{1}{2}, \beta = -\frac{1}{2}$ $a = \frac{\lambda}{2} + \frac{\mu}{\gamma}$
$\alpha = -\frac{1}{2}, \beta = \frac{1}{2}$ $a = \frac{\lambda}{2} + \frac{\gamma-1}{\gamma} \mu$	$\alpha = \beta = \frac{1}{2}$ $a = \frac{\lambda}{2} + \mu$

with the conditions (39) on  $a$ . The graphical results also hold with the ordinate replaced by  $\lambda/2$ .

These stability conditions have been verified computationally, and it has been shown that the stability of the systems is very sensitive to these conditions.

When shocks are involved the above conditions must be satisfied, but also  $\lambda$  must be large enough to prevent cell boundaries from crossing. Thus far no analysis is known in this connection and we must rely upon experimentation. In Chapter V where some additional adjustments in the stability criterion are considered, an example indicating the character of the required lower limit on  $\lambda$  will be given.



## CHAPTER IV

### DIFFERENCING PROCEDURES INVOLVING THE INTERNAL ENERGY CALCULATION

In practical applications of the Lagrangian difference equations, there has been some interest in the use of the energy equation in the form which gives the internal energy directly. The reason is the economy of calculations that results. Rather than evaluating both total and kinetic energies to obtain the internal energy, it is obtained directly. An additional advantage is that in some formulations the interpolations need not be carried out in the calculation procedure. Thus a worthwhile reduction in the number of mathematical manipulations is realized.

We proceed with a test of the system of equations (15), (16), and (3), with the energy equation (17) replaced by an internal energy calculation. The differential equation and a first possible difference form are

$$\frac{\partial I}{\partial t} = -P \frac{\partial u}{\partial x} \longrightarrow \frac{I_j^{n+1} - I_j^n}{\Delta t} = -P_j^n \frac{u_{j+\frac{1}{2}}^n - u_{j-\frac{1}{2}}^n}{m_j}$$

Solved for the internal energy at the advanced time, this is

$$I_j^{n+1} = I_j^n + P_j^n \frac{u_{j-\frac{1}{2}}^n - u_{j+\frac{1}{2}}^n}{m_j} \Delta t \quad (41)$$

where again

$$u^n = \frac{u^{n+\frac{1}{2}} + u^{n-\frac{1}{2}}}{2}$$

We now compare (41) with

$$I_j^{n+1} = I_j^n + P_j^n \frac{u_{j-\frac{1}{2}}^{n+\frac{1}{2}} - u_{j+\frac{1}{2}}^{n+\frac{1}{2}}}{m_j} \Delta t \quad (42)$$

From the conclusions reached in the preceding chapters regarding the time index on  $u$ , we exclude the case  $n = \frac{1}{2}$ .

For computational comparisons of these two forms of the energy equation, the same initial conditions were again used. [For details of the calculation refer to Table 2].\* Typical profiles of the internal energy in the initially-cold material are given in Figure 4. The analytic result is included for comparison. Form (42) gave results which are seriously in error, whereas form (41) matched the analytic solution except for fluctuations. Examination of the other field variables likewise

---

\* It will be noted upon examination of the character of equations (41) and (42) that if a cell  $j$  is initially cold, it will remain so indefinitely with the form of  $q$  of equation (18). To perform tests of these equations it was necessary to modify  $q$  to permit starting conditions. This was done here by replacing  $C_j^n$  in  $q$  by

$$\frac{C_j^n + |u_j^n - u_0|}{2}$$

where  $u_0$  is the velocity ahead of the shock layer. This modification does not affect the qualitative feature of the results in terms of the discussion here given. The predominant effects of this modified  $q$  are that starting conditions are provided or augmented, and additional damping of shock-produced fluctuations is realized.

showed correct results with (41) and incorrect results with (42). In particular it is evident in late time plots that the shock speed in the case of (42) is lower than the theoretical value.

The reason for the poor behavior of (42) may best be understood by an examination of the corresponding total and kinetic energy expressions. It can be shown that form (41), which gave correct results, is derivable from the energy equation (19) with the momentum equation (15) and interpolation formula (7). It is required, however, that the cell specific kinetic energy be defined by

$$\frac{u_j^2}{2} \equiv \frac{u_{j-\frac{1}{2}}^2 + u_{j+\frac{1}{2}}^2}{4} \quad (43)$$

rather than through the interpolation formula (8); that is, the cell center velocity is defined through an average of the cell boundary kinetic energies rather than an average of the boundary velocities. Of importance, however, is that the kinetic energy of the cell depends only upon the cell boundary velocities at the particular time in question. By contrast an analogous derivation of equation (42) is possible using equations (20), (15), and (7), but in this case the required defining formula for the kinetic energy is

$$\left(\frac{u_j^2}{2}\right)^{n+\frac{1}{2}} \equiv \left(\frac{u_{j-\frac{1}{2}}^2 + u_{j+\frac{1}{2}}^2}{2}\right)^{\frac{1}{2}} + \sum_{n'=1}^n \left[ \left(\frac{u_{j-\frac{1}{2}}^2 + u_{j+\frac{1}{2}}^2}{2}\right)^{n'+\frac{1}{2}} - \frac{u_{j-\frac{1}{2}}^{n'+\frac{1}{2}} u_{j-\frac{1}{2}}^{n'-\frac{1}{2}}}{2} - \frac{u_{j+\frac{1}{2}}^{n'+\frac{1}{2}} u_{j+\frac{1}{2}}^{n'-\frac{1}{2}}}{2} \right] \quad (44)$$

where the index  $1/2$  on the first term on the right is a time index. Note that this definition of the cell kinetic energy is in terms of the cell boundary velocities but involves all prior times to the time of interest.

To analyze the significance of the difference in the above required definitions of the kinetic energy, we diverge briefly to consider the meaning of conservation in a finite difference scheme. Since we are considering a net of points of information, the idea of conservation may be resolved to the requirement that the value of flux of momentum and energy remain the same whether observed in connection with the cell to the left or the cell to the right. Likewise the value of a given conservative variable specified at half-integer times must remain the same whether observed in connection with time earlier or later than the specified time. That is, conservation is equivalent to the requirement that single-valuedness of the variables exist at all points of the mesh. In our present discussion the temporal criterion is satisfied in regard to the kinetic energy, since it is uniquely defined at the net point  $j, n + \frac{1}{2}$  by equation (44). The problem, however, is that when shocks are involved, the Rankine-Hugoniot equations must be satisfied for the jump in the field variables at the shock. The Rankine-Hugoniot equations are statements of conservation of mass, momentum, and energy across the shock front. Since the shock is a local variation, these equations require local conservation. Local conservation of energy requires definitions of kinetic and internal energies in terms of local quantities. Thus in equation (44) the summed terms should not be

present. We note that the difference in the kinetic energies at two adjacent times is given by

$$\frac{\left(u_j^2\right)^{n+\frac{1}{2}}}{2} - \frac{\left(u_j^2\right)^{n-\frac{1}{2}}}{2} = \frac{\left(u_{j-\frac{1}{2}}^2 + u_{j+\frac{1}{2}}^2\right)^{n+\frac{1}{2}}}{2} - \frac{u_{j-\frac{1}{2}}^{n+\frac{1}{2}} u_{j-\frac{1}{2}}^{n-\frac{1}{2}} + u_{j+\frac{1}{2}}^{n+\frac{1}{2}} u_{j+\frac{1}{2}}^{n-\frac{1}{2}}}{2}$$

Hence in a local sense the kinetic energy as observed from time  $n - 1$  at time  $n - \frac{1}{2}$  is given by

$$\frac{\left(u_j^2\right)^{n-\frac{1}{2}}}{2} = \frac{\left(u_{j-\frac{1}{2}}^2 + u_{j+\frac{1}{2}}^2\right)^{n-\frac{1}{2}}}{2}$$

and as observed from time  $n$  is given by

$$\frac{\left(u_j^2\right)^{n-\frac{1}{2}}}{2} = \frac{u_{j-\frac{1}{2}}^{n+\frac{1}{2}} u_{j-\frac{1}{2}}^{n-\frac{1}{2}} + u_{j+\frac{1}{2}}^{n+\frac{1}{2}} u_{j+\frac{1}{2}}^{n-\frac{1}{2}}}{2}$$

Thus it is seen that locally the kinetic energy is not single-valued (that local conservation does not exist), and hence the Rankine-Hugoniot equations are not satisfied.

From this discussion we see that it is important that the form of the finite difference expressions be founded upon local definitions of those quantities which must be conserved. This can be achieved in the present discussion by beginning with a system of difference equations which involves a total energy calculation. In such a case an explicit definition of the kinetic energy must be made, and hence the requirement of local definition may be imposed. Such a system of equations may

then be used in deriving short-cut procedures.

Although no problems of the type discussed above arose in the present formulation of the momentum equation, the same considerations apply to it in general.

We now wish to examine some examples of internal energy calculations based upon the total energy equations given in the foregoing discussion. There are a number of possibilities, but we will consider only four of them. These four differ in the time index on  $u$  and in the kinetic energy interpolation used. We may tabulate these cases with  $n$  or  $n + \frac{1}{2}$  specifying the time index on  $u$  in the total energy equation, and (8) or (43) specifying the kinetic energy interpolation formula. Thus we designate

$$(a) \quad n, \quad (8)$$

$$(b) \quad n, \quad (43)$$

$$(c) \quad n + \frac{1}{2}, \quad (8)$$

$$(d) \quad n + \frac{1}{2}, \quad (43)$$

In all cases the boundary-pressure interpolation formula is equation (7), and the time index  $n + \frac{1}{2}$  on  $u$  is used in the position computation.

The derived internal energy equations are

$$(a) \quad I_j^{n+1} = I_j^n + \frac{\Delta t}{m_j} \left[ (P^n u^n)_{j-\frac{1}{2}} - (P^n u^n)_{j+\frac{1}{2}} - u_j^n (P_{j-\frac{1}{2}}^n - P_{j+\frac{1}{2}}^n) \right]$$

$$(b) \quad I_j^{n+1} = I_j^n + \frac{\Delta t}{m_j} P_j^n (u_{j-\frac{1}{2}}^n - u_{j+\frac{1}{2}}^n)$$

$$(c) \quad I_j^{n+1} = I_j^n + \frac{\Delta t}{m_j} \left[ (P_u^{n+\frac{1}{2}})_{j-\frac{1}{2}} - (P_u^{n+\frac{1}{2}})_{j+\frac{1}{2}} - u_j^n (P_{j-\frac{1}{2}}^n - P_{j+\frac{1}{2}}^n) \right]$$

$$(d) \quad I_j^{n+1} = I_j^n + \frac{\Delta t}{m_j} P_j^n \left( u_{j-\frac{1}{2}}^{n+\frac{1}{2}} - u_{j+\frac{1}{2}}^{n-\frac{1}{2}} \right) + \frac{1}{4} \left[ \left( a_{j-\frac{1}{2}}^n \right)^2 + \left( a_{j+\frac{1}{2}}^n \right)^2 \right] \Delta t^2$$

The index  $n$  on  $u$  wherever it appears again means

$$u^n = \frac{u^{n+\frac{1}{2}} + u^{n-\frac{1}{2}}}{2}$$

In (d) the acceleration  $a_{j-\frac{1}{2}}^n$  is given by

$$a_{j-\frac{1}{2}}^n = \frac{P_{j-1}^n - P_j^n}{\frac{1}{2}(m_{j-1} + m_j)}$$

We have introduced only one new difference form, (d). (a) and (c) were discussed in Chapter II where they appeared as equations (19) and (20), respectively. (b) is equation (41) repeated here for comparison.

Note that the new form (d) without the last term is just equation (42). The second order term in  $\Delta t$  added to (42) resulted from our definition of the kinetic energy in terms of local quantities (equation 43).

Of passing interest we note that (a) and (c) are difference approximations to

$$\frac{\partial I}{\partial t} = - \left[ \frac{\partial(Pu)}{\partial m} - u \frac{\partial P}{\partial m} \right]$$

They differ only in the time index on  $u$  in the work flux at the cell boundaries. In Chapter II we concluded that (c) was a superior form to

use in that it led to smoother profiles for a given  $q$  and  $\Delta t$  (refer to Figure 3). Likewise, while the stability conditions for (a) were not given in Chapter III, the trend indicated that the most advanced time required the least compensation of errors in terms of the magnitude of  $q$ . The stability conditions for (c) and (d) are the same and are the  $\alpha = \beta = -1/2$  case discussed in Chapter III. (a) and (b) correspond to  $\alpha = 1/2, \beta = 0$  in the notation there used. Differences in the form of the kinetic energy interpolation formula vanish when the equations are linearized, thus leading to identical stability conditions through the type of analysis of Chapter III.

To further check the assumption that the more advanced time on  $u$  gives superior results, forms (b) and (d) were compared using the same initial conditions of previous tests. [For details of this test refer to Table 2]. For this comparison typical density profiles are given in Figure 5 along with the analytic result. Again we ignore the error in the cells near the energy source material and make the comparison on relative smoothness of the profiles. We note that (d) tends to take on mean values of (b) and is therefore considered to be superior.

To take further advantage of the advanced time on  $u$ , it might be suggested that  $u_j^n$  in form (c) be replaced by  $u_j^{n+\frac{1}{2}}$ . This, however, leads back to the problem of the kinetic energy being defined in terms of non-local quantities.

A comparison of (c) and (d) is of some interest. Although these forms are the same in terms of first variations, they differ in second



order. Form (c) differs from (d) in that the kinetic energy is always less by a factor

$$\frac{(u_{j-\frac{1}{2}} - u_{j+\frac{1}{2}})^2}{8}$$

This reduction in kinetic energy goes into internal energy and hence results in an entropy increase. This term has most significance where the velocity gradients are large and thus acts as an auxiliary viscosity in shock regions; as would be expected, it helps to prevent cell boundaries from crossing as a result of shocks.

It will be noted that in an adiabatic rarefaction the term will cause an entropy increase since it will remain positive. Although this effect may be small, it is still undesirable. It is therefore recommended that if the characteristics of form (c) are otherwise desirable, the above term should be taken into account only in cells for which  $u_{j-\frac{1}{2}} - u_{j+\frac{1}{2}} > 0$ , as has been specified for q. This is equivalent to using form (d) normally, but replacing it by form (c) in compressive regions. The merits of form (c) may perhaps more easily be realized by modifying q as suggested by Landshoff,<sup>3</sup> that is, by adding a term to q involving  $(\Delta u)^2$ . Doing this will provide the same effect in isothermal regions as well.

## CHAPTER V

### DISCUSSION OF ERRORS

Whereas the difference methods presented in the previous chapters give satisfactory results in most problem situations, there are errors evident in all cases which stem from the artificially introduced diffusion term, i.e., from the use of the mechanism  $q$ . We will first note the form these errors take in some sample results.

In Figure 6 a density profile of differencing form (c) is given. Reference to Table 3 shows that this test was made with equal mass zones. That is, the light isothermal material had large cells, while the initially cold, heavy material had relatively small cells. The tests were made in this way to minimize the truncation error in the mass derivatives at the material interface. In contrast, a corresponding test (c-4) was made in which cell sizes were more of the same order [refer to Table 4]. The density profile of this test is also given in Figure 6.

The phenomenon of interest is the low density relative to the theoretical value that occurs in the first few cells of the shocked material. In the case of the cells of equal mass, the effect is spread over several

cells, while in the case of cells more equal in physical size, the effect is more severe but confined to the first two cells.

In Figure 7 the internal energy profiles of the shocked material are given for the same tests. Note that the effect under consideration is here manifested in an excess of internal energy in the first cells.

In Figure 8 velocity profiles in the rarefaction region of the isothermal material are presented along with the theoretical curve. [Refer to Table 5 for details of this test]. The solid-line curve corresponds to tests of difference form (c) with  $q$  restricted to compressed cells, while the dashed curve is a result in which  $q$  was unrestricted, i.e.,  $q$  took on both positive and negative values. We first note that both experimental curves lag behind the theoretical curve. This, however, is of no concern since the lag is related to starting conditions and does not grow in time. We note, however, that the unrestricted  $q$  causes an unrealistic spread in the rarefaction front. This incidentally is the reason that the restricted  $q$  is generally used. Further, it is noted that while the restricted  $q$  curve has the correct velocity gradient in the rarefaction fan, there is a rise in the velocity immediately behind the rarefaction. This is not a consequence of  $q$  in the vicinity of the rarefaction fan; in fact,  $q$  is instrumental in reducing a larger rise in velocity in this region that would be present without the viscosity. We must therefore relate this effect with errors that occurred at the origin of the disturbance.

Finally, Figure 9 shows a density profile of the differencing types

(c) and (d) of Chapter IV applied to a shock moving into a material discontinuity where the material on the left is more dense by a factor of 25 [refer to Table 6 for details of this test]. When the shock strikes the material discontinuity, a shock moves into the light material on the right and a rarefaction moves into the more dense material on the left. The errors that are here evident, relative to the theoretical curve, may be correlated to the effects pointed out above. Again the density in the first cells of the shocked material is low. The excessive velocity behind the rarefaction fan is manifested as a region of lower density than the theoretical value. The high peak in the density at the material interface in the rarefied material is merely a consequence of the oversized cells to the right.

From the above examples and discussion it is apparent that the major errors may be correlated with effects occurring at material discontinuities. The low density and high internal energy occurring in the first cells of the shocked material is discussed briefly by Landshoff.<sup>3</sup> This effect is attributed to an overproduction of entropy in the affected cells, resulting in excessive heating and a consequent expansion of these cells. It is therefore related to the character of the dissipative mechanism  $q$ . Since the peculiarities connected with rarefactions were traced back to where the rarefaction originated, then these errors likewise are assumed to be a consequence of the action of  $q$  at material discontinuities.

Although an artificial viscosity is essential to the type of treatment here given to shocks, its secondary effects can become of some

concern. Basically,  $q$  was manufactured to effect a replacement of a steady state shock by a shock layer of thickness on the order of a cell size. The process of development or modification of this layer is not provided for in the character of  $q$ . The errors evident in Figures 6 and 7 are correlated with the development of the shock layer from initial conditions, while in Figure 9 the shock layer required modification at the material interface.

Experiments in which the viscosity coefficient  $\lambda$  was changed show that a larger  $\lambda$  increases the entropy production at material discontinuities and hence increases the errors. Modification of  $\lambda$  alone, however, is not sufficiently effective to eliminate the errors. A balance must be achieved in the size of  $\lambda$ , in which the further considerations of fluctuations and crossing of boundaries must be considered.

In Chapter III it was pointed out that the stability conditions of the equations required modification when shocks were involved;  $\lambda$  must be sufficiently large to prevent boundaries from crossing. An additional modification is required because of the secondary effects of  $q$  discussed above.

In Figure 10 experimental points are plotted for difference form (d) with the initial conditions of Table 7. These points are superimposed upon the previously discussed plot of the region of stability for difference forms  $\alpha = \beta = 1/2$ , in which  $q$  is the restricted form. The results must be taken only in a qualitative sense, since boundary crossing is strongly dependent upon initial conditions. The points of

instability resulting from shocks are classified into two groups. Boundary crossings occurred after only a few time steps and involved the interface between the isothermal material and the initially cold material. Instabilities arising from the overproduction of entropy occurred at relatively late times and were effective in the region directly following the cells in which the low density errors occurred. This latter type of instability depends upon the relative cell sizes of the two materials of the interface. If the cells of the isothermal material were larger, this type of instability would be less likely to arise because the low density errors would be less severe [refer to Figures 6 and 7]. Note that for the type of instability considered, improvement with reduced  $\lambda$  is small. The present point of view is that the secondary effects of  $q$  are such as to modify the condition

$$\frac{\delta u}{\delta x} \delta t < 1$$

or

$$\mu < \frac{C}{(\delta u / \delta x) \delta x}$$

which certainly must be satisfied for compressed cells.

In Chapter III it was noted that a shift in the region of stability to lower values of  $\lambda$  was a qualitative indication that the difference form was superior. The question might be raised, why then use a restricted  $q$  which shifts the region of stability to  $\lambda$ 's of twice the value of the unrestricted  $q$ ? If a technique could be devised to prevent the appearance of  $q$  in rarefactions, but still retain it in unrestricted form in all other regions, then an improvement could be realized.

#### REFERENCES

1. Harlow, F. H., "Dynamics of Compressible Fluids," Los Alamos Scientific Laboratory Report LA-2412 (April 1960), Chapter I.
2. Richtmyer, R. D., "Difference Methods for Initial-Value Problems," Interscience Publishers, Inc., New York, 1957, Chapter X.
3. Landshoff, R., "A Numerical Method for Treating Fluid Flow in the Presence of Shocks," Los Alamos Scientific Laboratory Report LA-1930 (January 1955).
4. Harlow, F. H., "Stability of Difference Equations — Selected Topics," Los Alamos Scientific Laboratory Report LAMS-2452 (July 1960).

TABLE 1

INITIAL CONDITIONS FOR CALCULATIONS SHOWN IN FIG. 1

 $\Delta t$  fixed at 0.0625

Material No.	1 (isothermal)	2
$\gamma$	$5/3$	$5/3$
$m_j$	1	1
$\rho_j$	0.1	1
$I_j$	0.246	0
$\lambda$	$1/\gamma$	$1/\gamma$



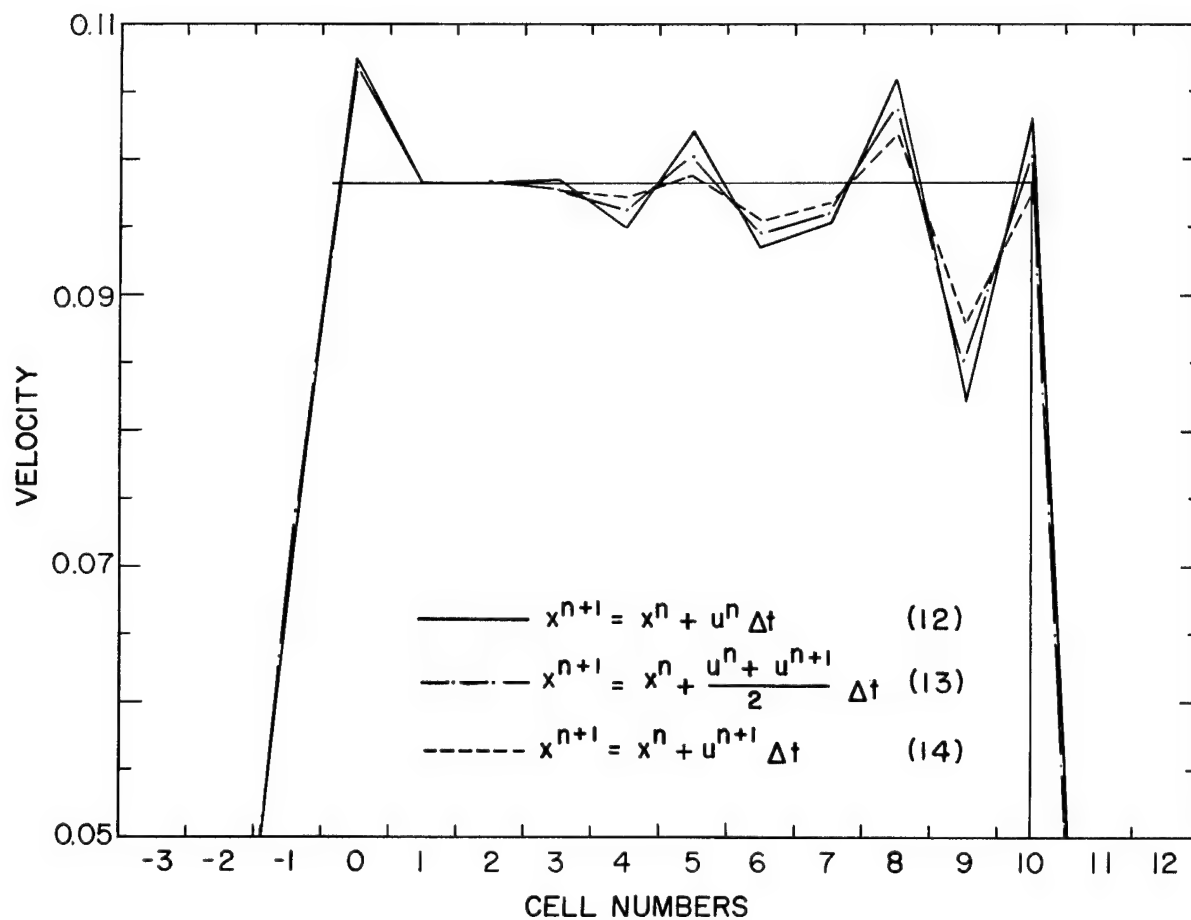


Fig. 1: First test of Chapter II. Cell velocity profile at time  $t = 15$ . Cells 0, -1, -2, etc., are larger than cells to right by a factor of 10. [Refer to Table 1].

TABLE 2

INITIAL CONDITIONS FOR CALCULATIONS SHOWN IN FIGS. 2, 3, 4, and 5\*

$$\Delta t \text{ adjusted to satisfy } \left( \frac{c}{\Delta x} \right)_{\max} \Delta t < 1$$

Material No.	1 (isothermal)	2
$\gamma$	5/3	5/3
$m_j$	1	1
$\rho_j$	0.1	1
$I_j$	0.246	0
$\lambda$	1/ $\gamma$	1/ $\gamma$

\*Refer to footnote Page 36 in connection with Figs. 4 and 5.

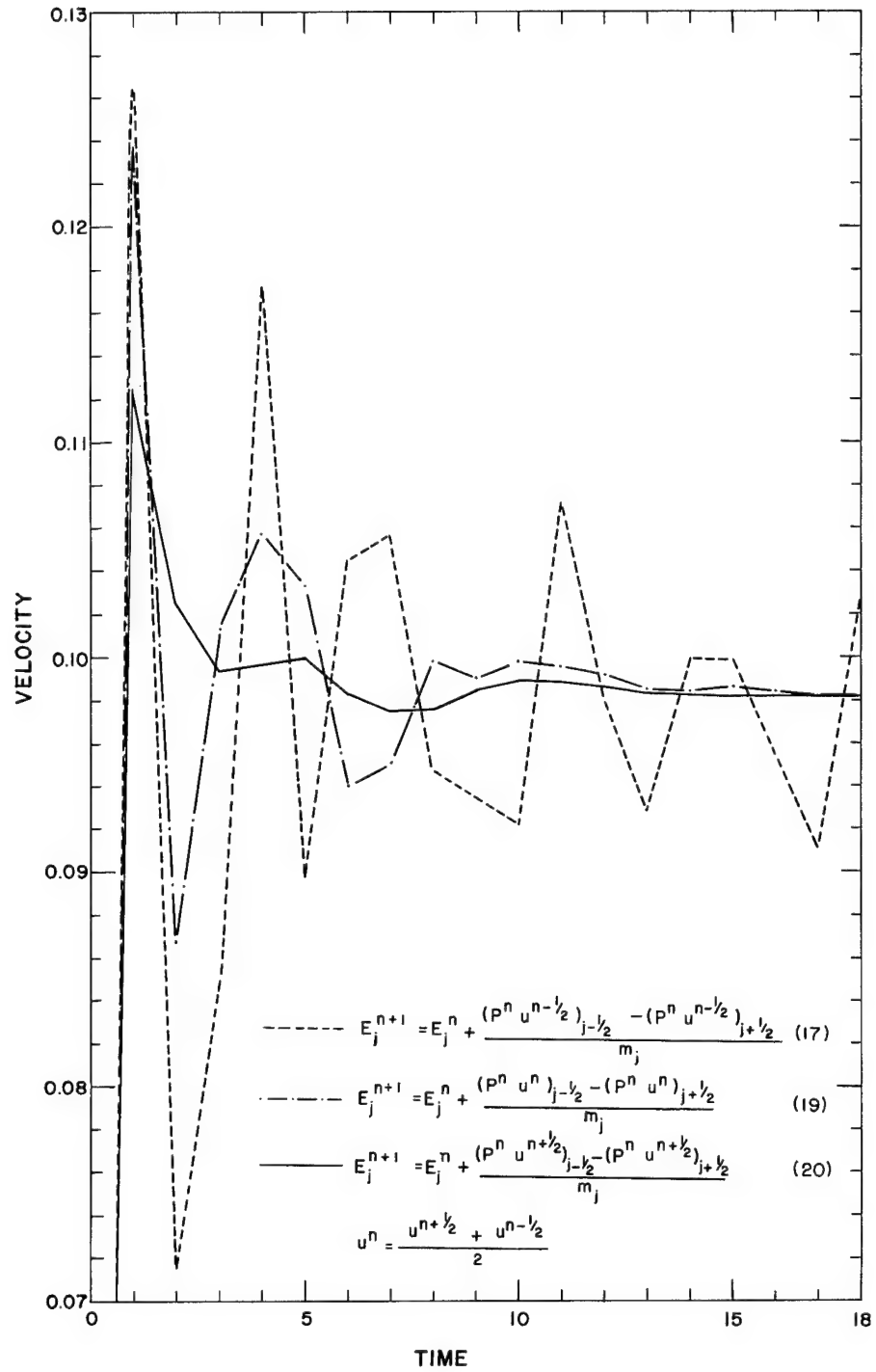


Fig. 2: Second test of Chapter II. Material interface velocity as a function of time. [Refer to Table 2].

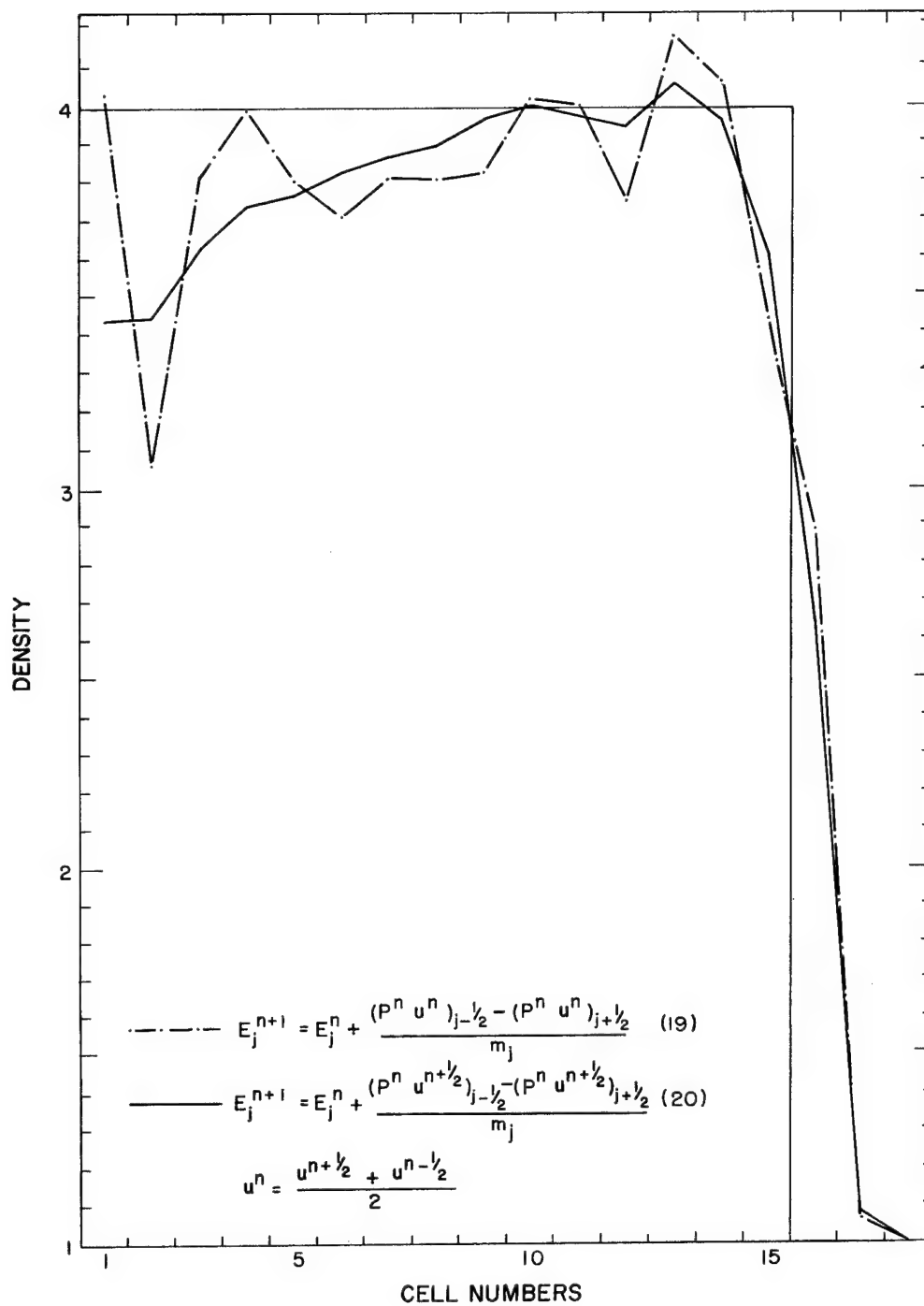


Fig. 3: Second test of Chapter II. Density profile of material 2 at time  $t = 15$ . [Refer to Table 2].

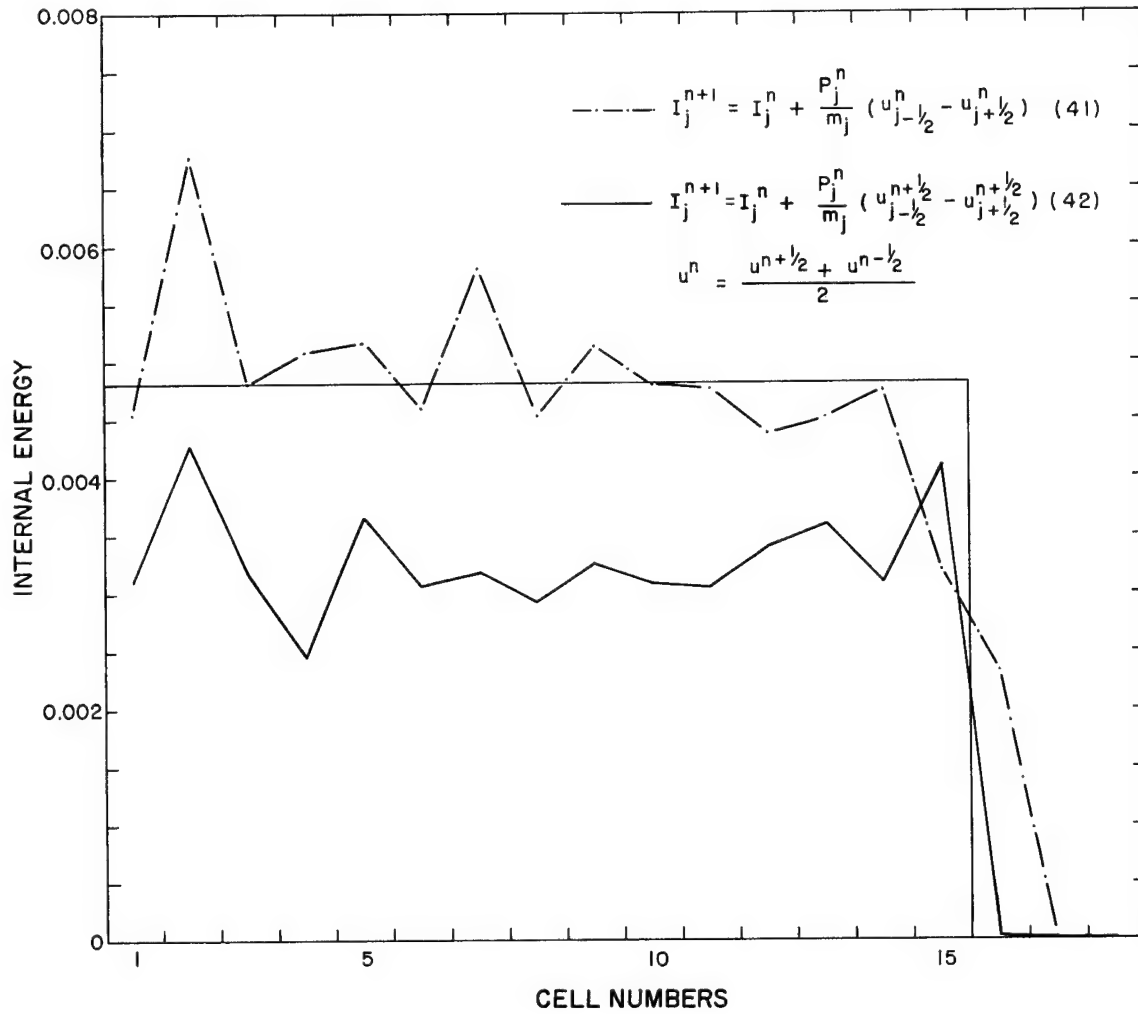


Fig. 4: Chapter IV test. Internal energy profile of material 2 at time  $t = 15$ . [Refer to Table 2].

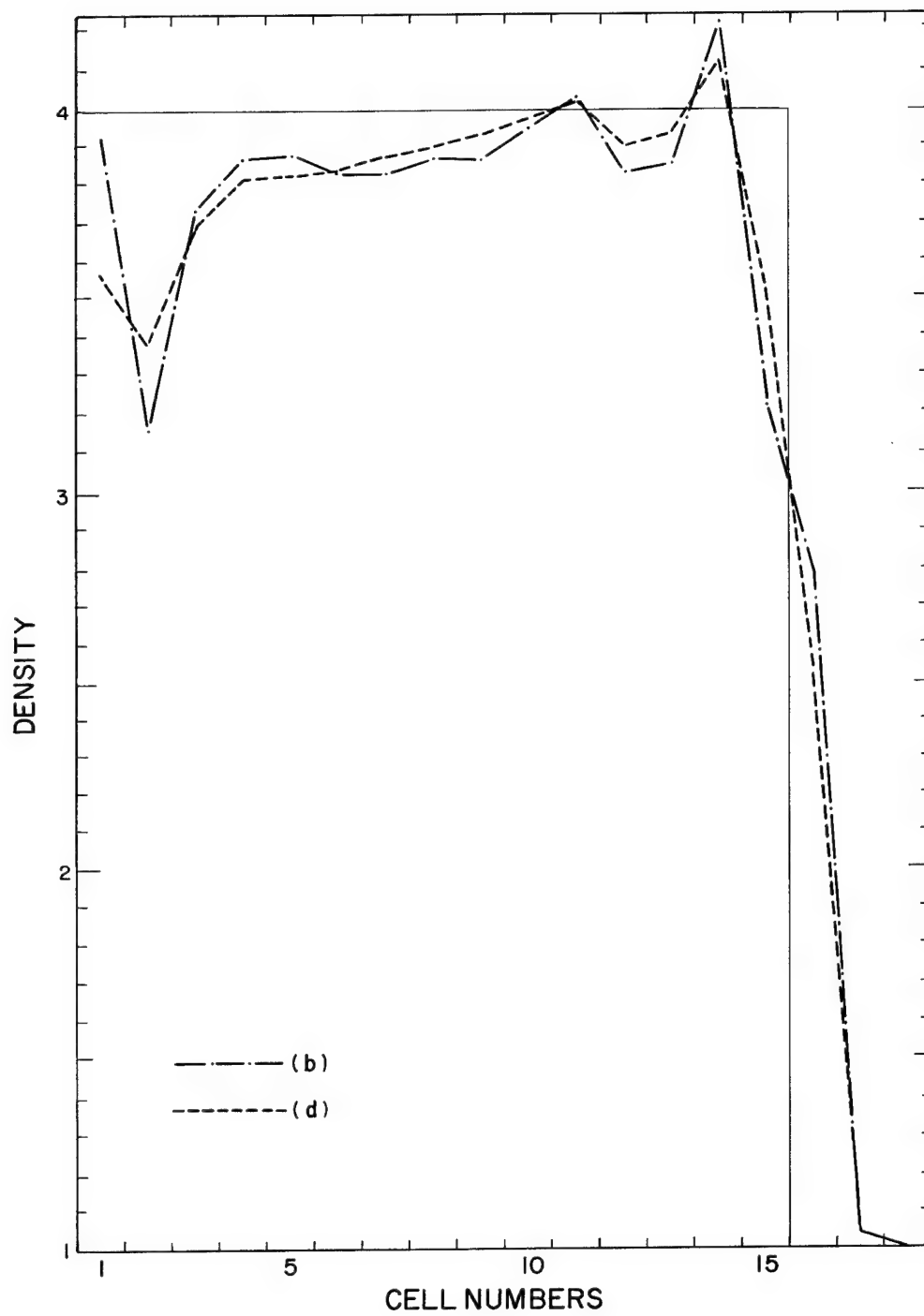


Fig. 5: Chapter IV test. Density profile of material 2 at time  $t = 15$ .  
[Refer to Table 2].

TABLE 3

INITIAL CONDITIONS FOR CALCULATION (c) SHOWN IN FIGS. 6 AND 7

$$\Delta t \text{ adjusted to satisfy } \sqrt{6} \left( \frac{c}{\Delta x} \right)_{\max} \Delta t < 1$$

Material No.	1 (isothermal)	2
$\gamma$	5/3	5/3
$m_j$	1	1
$\rho_j$	0.1	1
$I_j$	0.246	0
$\lambda$	1/ $\gamma$	1/ $\gamma$

TABLE 4

INITIAL CONDITIONS FOR CALCULATION (c-4) SHOWN IN FIGS. 6 AND 7

$$\Delta t \text{ adjusted to satisfy } \sqrt{6} \left( \frac{c}{\Delta x} \right)_{\max} \Delta t < 1$$

Material No.	1 (isothermal)	2
$\gamma$	5/3	5/3
$m_j$	0.14	1
$\rho_j$	0.1	1
$I_j$	0.246	0
$\lambda$	1/ $\gamma$	1. $\gamma$

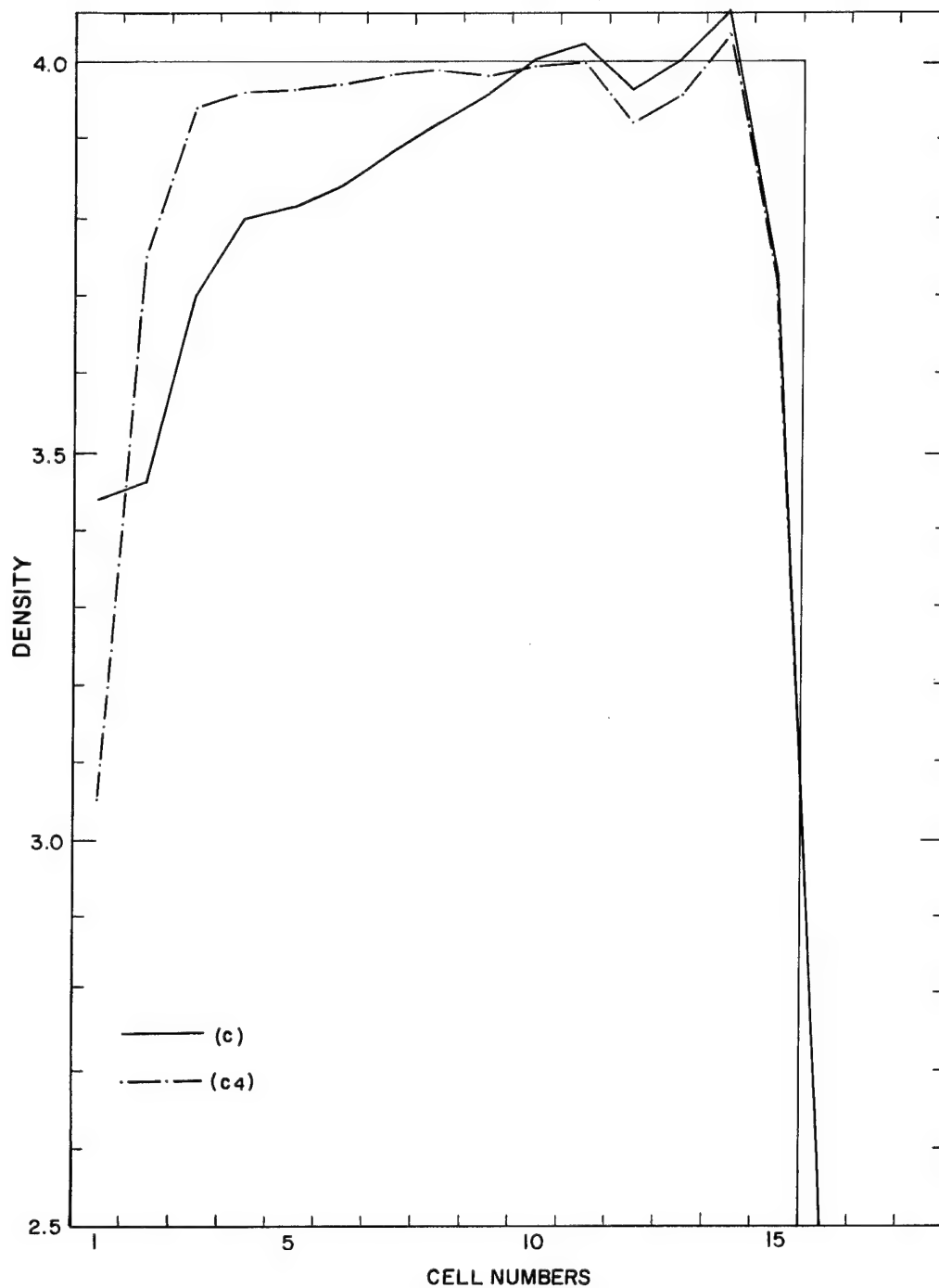


Fig. 6: Chapter V error illustration. Density profiles of material 2 taken for different initial cell sizes in material 1 ( $t = 15$ ). [Refer to Tables 3 and 4].



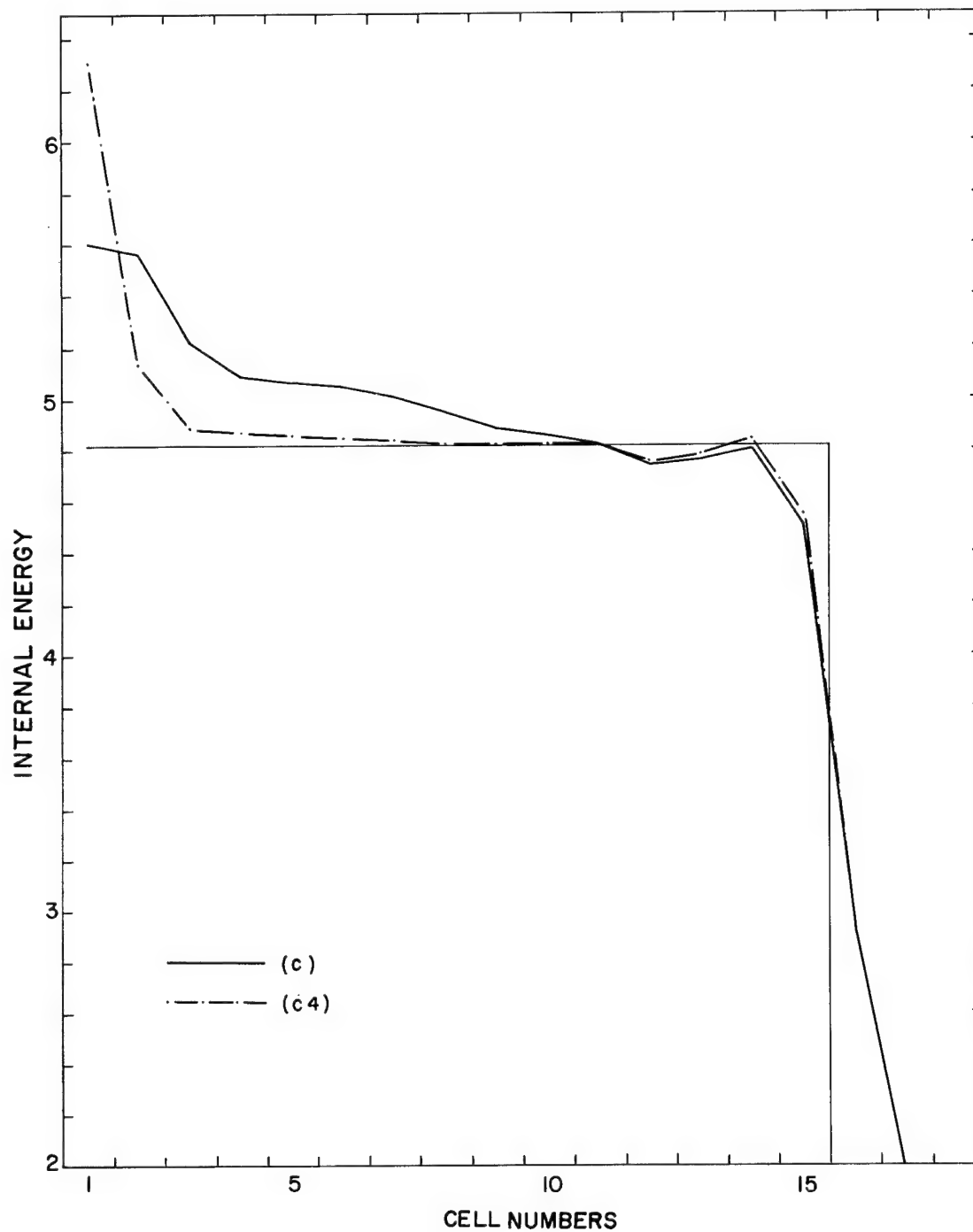


Fig. 7: Chapter V error illustration. Internal energy profiles of material 2 taken for different initial cell sizes in material 1 ( $t = 15$ ). [Refer to Tables 3 and 4].

TABLE 5

INITIAL CONDITIONS FOR CALCULATIONS SHOWN IN FIG. 8

$$\Delta t \text{ adjusted to satisfy } \sqrt{6} \left( \frac{c}{\Delta x} \right)_{\max} \Delta t < 1$$

Material No.	1 (isothermal)	2
$\gamma$	$5/3$	$5/3$
$m_j$	0.25	1
$\rho_j$	0.1	1
$I_j$	0.246	0
$\lambda$	$1/\gamma$	$1/\gamma$

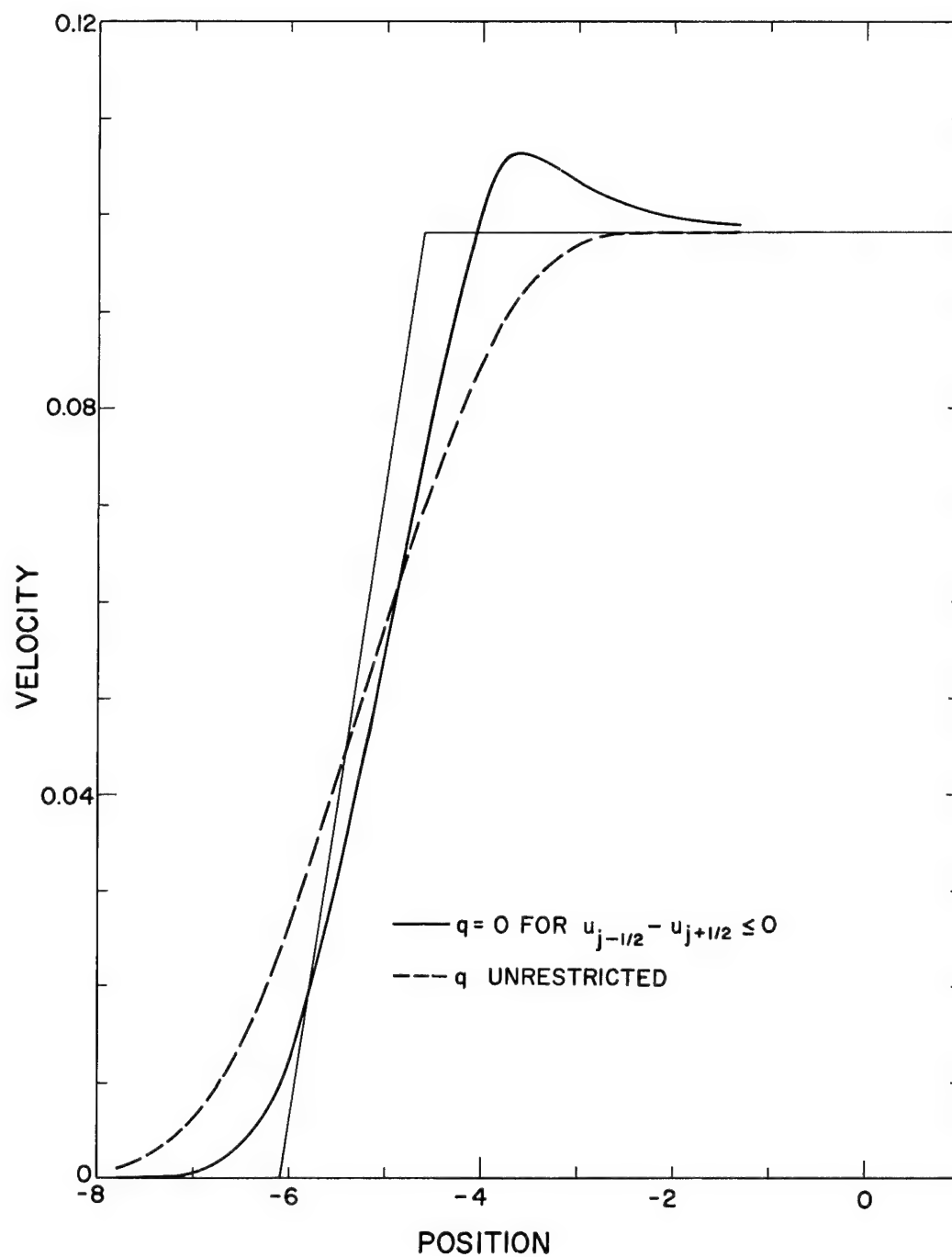


Fig. 8: Chapter V error illustration. Velocity profiles in material 1 comparing two forms of  $q$  in the rarefaction ( $t = 15$ ). [Refer to Table 5].

TABLE 6

INITIAL CONDITIONS FOR CALCULATIONS SHOWN IN FIG. 9\*

$$\Delta t \text{ adjusted to satisfy } \sqrt{6} \left( \frac{c}{\Delta x} \right)_{\max} \Delta t < 1$$

Material No.	1 (isothermal)	2	3
$\gamma$	5/3	5/3	5/3
$m_j$	0.25	1	0.2
$\rho_j$	0.1	1	.04
$I_j$	0.246	0	0
$\lambda$	1/ $\gamma$	1/ $\gamma$	1/ $\gamma$

\*The form of  $q$  described in the footnote of page 36 was used here. It should be noted, however, that neither form (c) nor (d) require starting conditions.

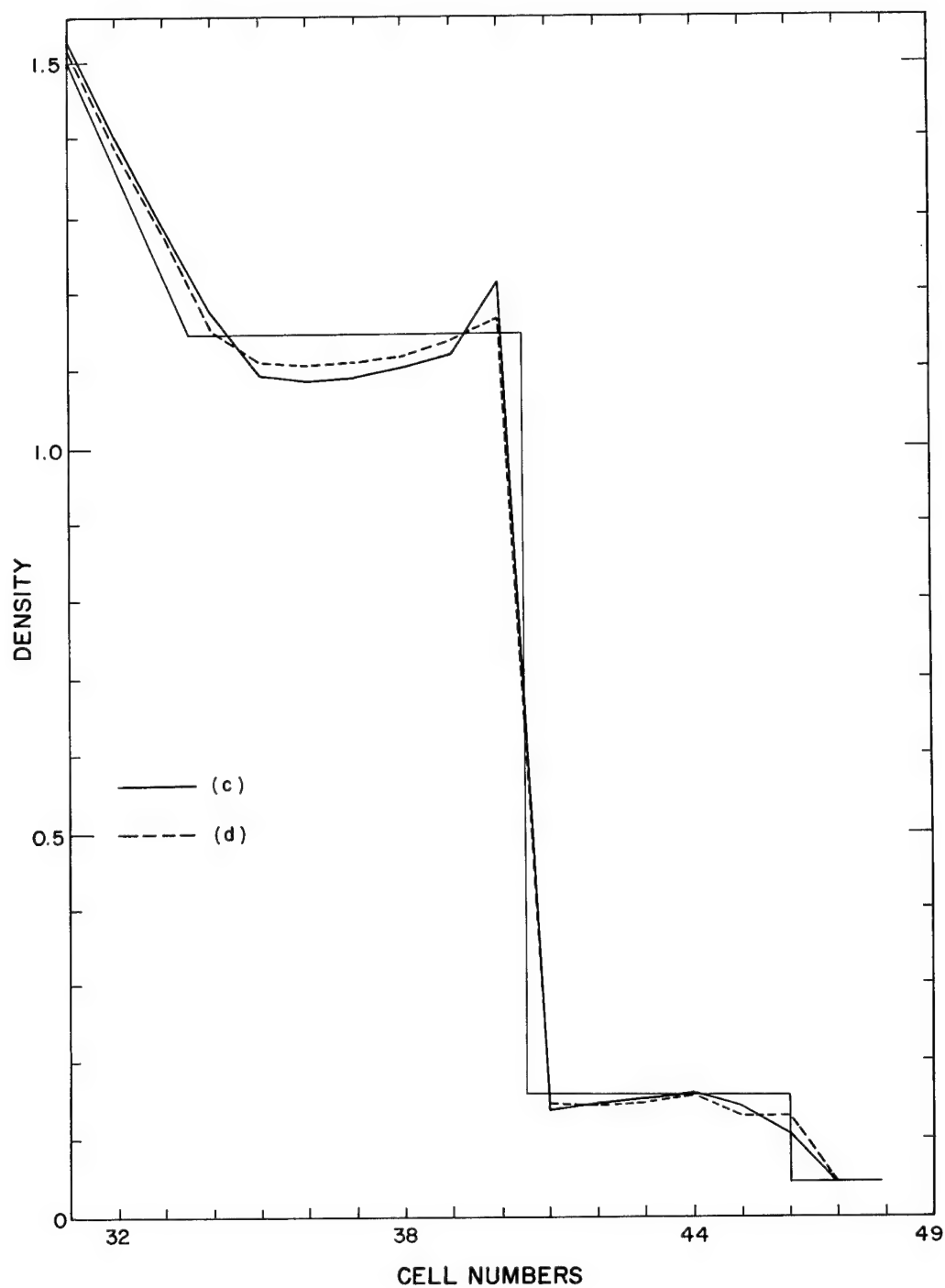


Fig. 9: Chapter V error illustration. Density profiles at time  $t = t_0 + 15.9$ , where  $t_0$  is time shock passed the second material interface. [Refer to Table 6].

TABLE 7

INITIAL CONDITIONS FOR CALCULATIONS USED IN CONNECTION WITH FIG. 10

 $\lambda$  and  $\mu$  (fixed  $\Delta t$ ) as indicated on Fig. 10

Material No.	1 (isothermal)	2
$\gamma$	$5/3$	$5/3$
$m_j$	0.25	1
$\rho_j$	0.1	1
$I_j$	0.246	0

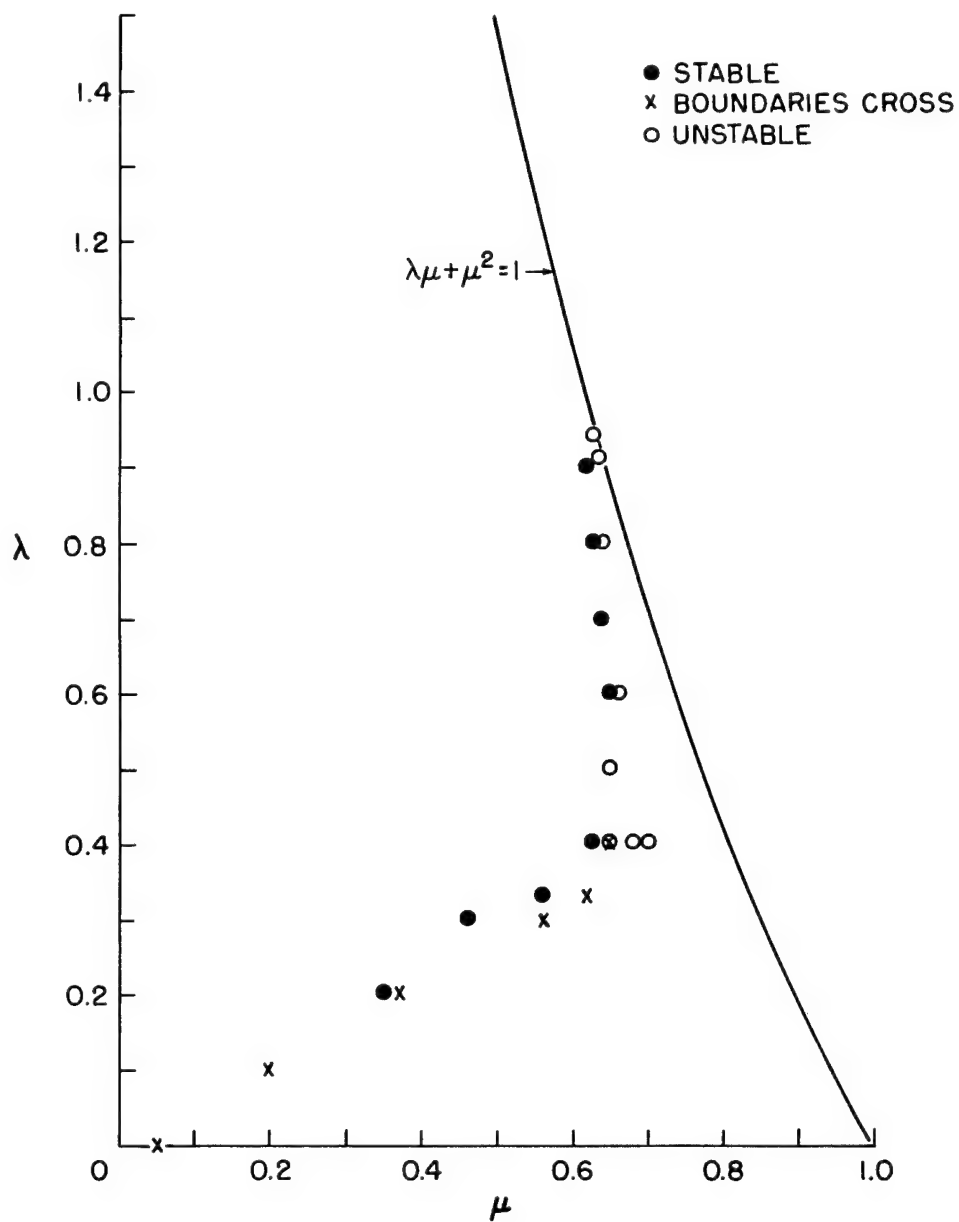


Fig. 10: Chapter V. Example of experimental points of stability and nonstability when shocks are involved. [Refer to Table 7].

## APPENDIX

### ENTROPY OF A REGION OF FLUID

Consider a one-dimensional region of a fluid which is subject to variations, the variations in turn being subject to the constraints of fixed mass, fixed momentum, and fixed energy. That is,

$$\begin{aligned}m &= \int_a^b \rho \, dx = \text{constant} \\M &= \int_a^b \rho \, u \, dx = \int_a^b \bar{M}(\rho, u) \, dx = \text{constant} \\E &= \int_a^b \rho \left[ I(\rho, P) + \frac{1}{2} u^2 \right] \, dx = \int_a^b \bar{E}(\rho, P, u) \, dx = \text{constant}\end{aligned} \tag{A-1}$$

where  $\bar{M}$  and  $\bar{E}$  are momentum and energy densities, respectively.

Now also let  $\bar{S}(\rho, P)$  be the entropy density of the fluid region such that the total entropy is given by

$$S = \int_a^b \bar{S} \, dx \tag{A-2}$$

We are interested in examining the character of extremal values of  $S$  in terms of variations of  $\rho$ ,  $P$ , and  $u$  which are arbitrary except for the specified conservative constraints. The condition for an extremal value of  $S$  is



$$dS = \int_a^b \left( \frac{\partial \bar{S}}{\partial \rho} \delta \rho + \frac{\partial \bar{S}}{\partial P} \delta P \right) dx = 0 \quad (A-3)$$

The constraints in terms of variations of  $\rho$ ,  $u$ , and  $P$  are

$$\int_a^b \delta \rho \, dx = 0$$

$$\int_a^b \left( \frac{\partial \bar{M}}{\partial \rho} \delta \rho + \frac{\partial \bar{M}}{\partial u} \delta u \right) dx = 0 \quad (A-4)$$

$$\int_a^b \left( \frac{\partial \bar{E}}{\partial \rho} \delta \rho + \frac{\partial \bar{E}}{\partial u} \delta u + \frac{\partial \bar{E}}{\partial P} \delta P \right) dx = 0$$

Multiplying these constraints successively by the Lagrangian multipliers  $f$ ,  $g$ , and  $h$  and adding to the equation  $dS = 0$ , we have

$$\begin{aligned} \int_a^b \left\{ \left[ \frac{\partial \bar{S}}{\partial \rho} + f + g \frac{\partial \bar{M}}{\partial \rho} + h \frac{\partial \bar{E}}{\partial \rho} \right] \delta \rho \right. \\ \left. + \left[ \frac{\partial \bar{S}}{\partial P} + h \frac{\partial \bar{E}}{\partial P} \right] \delta P + \left[ g \frac{\partial \bar{M}}{\partial u} + h \frac{\partial \bar{E}}{\partial u} \right] \delta u \right\} dx = 0 \end{aligned} \quad (A-5)$$

Since all the specified constraints are now included, the variations  $\delta \rho$ ,  $\delta P$ , and  $\delta u$  are arbitrary (i.e. independent); hence the coefficients of these variations must vanish individually. We thus have

$$\begin{aligned} \frac{\partial \bar{S}}{\partial \rho} + f + g \frac{\partial \bar{M}}{\partial \rho} + h \frac{\partial \bar{E}}{\partial \rho} \\ \frac{\partial \bar{S}}{\partial P} + h \frac{\partial \bar{E}}{\partial P} = 0 \\ g \frac{\partial \bar{M}}{\partial u} + h \frac{\partial \bar{E}}{\partial u} = 0 \end{aligned} \quad (A-6)$$

Through specification of material equations of state and the above definitions,  $\bar{S}$ ,  $\bar{M}$ , and  $\bar{E}$  become known functions of  $\rho$ ,  $P$ , and  $u$ . Hence the equations (A-6) reduce to a set of algebraic equations in the three unknowns  $\rho$ ,  $P$ , and  $u$  with solutions

$$\rho = \text{constant}$$

$$P = \text{constant}$$

$$u = \text{constant}$$

With the specified constraints governing the behavior of the region of fluid under consideration, we thus conclude that the entropy will have an extremal value characterized by a flat profile in all variables.

Since we have established what characterizes this extremal value of  $S$ , the examination of any other condition will tell us if the extremal is a maximum or a minimum.

Consider a small space variation in internal energy only, that is,

$$I = I_0 + \epsilon(x)$$

$$\rho = \rho_0 \tag{A-7}$$

$$u = u_0$$

Then the fixed energy constraint becomes

$$\int_a^b \rho_0 \left[ I_0 + \epsilon(x) + \frac{1}{2} u_0^2 \right] dx = \rho_0 \left[ I_0 + \frac{1}{2} u_0^2 \right] \int_a^b \epsilon(x) dx = 0$$

or

$$\int_a^b \epsilon(x) dx = 0 \tag{A-8}$$

The remaining two constraints are automatically satisfied since (A-7) specifies no variation in  $\rho$  and  $u$ . Also for this special case  $\bar{S} = \bar{S}(I)$  only, and

$$\bar{S} = \bar{S}_0 + \epsilon(x) \left( \frac{\partial \bar{S}}{\partial I} \right)_0 + \frac{\epsilon^2(x)}{2} \left( \frac{\partial^2 \bar{S}}{\partial I^2} \right)_0 + \dots$$

With equation (A-8) taken into account, the change in entropy of the region becomes

$$dS = \int_a^b (\bar{S} - \bar{S}_0) dx \approx \frac{1}{2} \left( \frac{\partial^2 \bar{S}}{\partial I^2} \right)_0 \int_a^b \epsilon(x)^2 dx$$

Note now that the established extremum of  $S$  is a maximum if  $(\partial^2 \bar{S} / \partial I^2)$  is negative definite. With the density constant the second law of thermodynamics states that

$$\left( \frac{\partial S}{\partial I} \right)_\rho = \frac{1}{T}$$

Hence

$$\left( \frac{\partial^2 \bar{S}}{\partial I^2} \right)_\rho = - \frac{1}{T^2} \left( \frac{\partial T}{\partial I} \right)$$

Now

$$\left( \frac{\partial T}{\partial I} \right)_\rho > 0$$

is a fundamental property of actual media, and therefore

$$\left( \frac{\partial^2 \bar{S}}{\partial I^2} \right)_\rho < 0$$

Thus we have shown that a flat profile of the variables characterizing the fluid implies an entropy maximum if the conservation laws hold.

Conversely, if we consider a true solution to the hydrodynamic equations characterized by some value of entropy and compare with it a finite difference approximation solution, then the degree of fluctuation in the approximation may be correlated with error terms contributing to a decrease in entropy. This is assuming that the difference approximation is conservative in the above specified quantities.